Geomechanics for Energy and the Environment 42 (2025) 100668

Contents lists available at ScienceDirect

Geomechanics for Energy and the Environment

journal homepage: www.elsevier.com/locate/gete

Numerical simulation of coupled THM behaviour of full-scale EBS in backfilled experimental gallery in the Horonobe URL

Yutaka Sugita [a,*], Hirokazu Ohno [a], Steffen Beese [b], Pengzhi Pan [c], Minseop Kim [d], Changsoo Lee [d], Carlos Jove-Colon [e], Carlos M. Lopez [e], Suu-yan Liang [f]

[a] Japan Atomic Energy Agency (JAEA), Horonobe, Hokkaido, Japan
[b] Federal Institute for Geosciences and Natural Resources (BGR), Hannover, Germany
[c] State Key Laboratory of Geomechanics and Geotechnical Engineering Safety, Institute of Rock and Soil Mechanics, Chinese Academy of Sciences (CAS), Wuhan, China
[d] Korea Atomic Energy Research Institute (KAERI), Daejeon, Republic of Korea
[e] Sandia National Laboratory (SNL), Albuquerque, NM, USA
[f] Sinotech Engineering Consultants, Inc. (Sinotech), Taipei, Taiwan

ARTICLE INFO

Keywords:
Coupled thermo-hydro-mechanical behaviour
Numerical simulation
Horonobe URL
DECOVALEX-2023
Engineered barrier system
Radioactive waste disposal

ABSTRACT

Bentonite-based engineered barrier system (EBS) is a key component of many repository designs for the geological disposal of high-level radioactive waste. Given the complexity and interaction of the phenomena affecting the barrier system, coupled thermo-hydro-mechanical (THM) numerical analyses are a potentially useful tool for a better understanding of their behaviour. In this context, a Task (the Horonobe EBS experiment) was undertaken to study, using numerical analyses, the thermo-hydro-mechanical (and thermo-hydro) interactions in bentonite based engineered barriers within the international cooperative project DECOVALEX 2023. One full-scale in-situ experiment and four laboratory experiments, largely complementary, were selected for modelling. The Horonobe EBS experiment is a temperature-controlled non-isothermal experiment combined with artificial groundwater injection. The Horonobe EBS experiment consists of the heating and cooling phases. Six research teams performed the THM or TH (depended on research team approach) numerical analyses using a variety of computer codes, formulations and constitutive laws. For each experiment, the basic features of the analyses are described and the comparison between calculations and laboratory experiments and field observations are presented and discussed.

1. Introduction

Deep geological repository systems for high-level radioactive waste (vitrified waste or spent nuclear fuel) are generally based on a multi-barrier (combination of engineered barrier and natural barrier) approach. The engineered barrier (e.g. metal overpack, buffer material) and the natural barrier (host rock) jointly contribute to an appropriate long-term confinement of the radio nuclides released from the radioactive waste. The bentonite-based engineered barrier (buffer material) is usually a key component of the deep geological repository designs for the radioactive waste. In the most general case, the engineered barrier is subject to complex interacting phenomena comprising the heat released from the radioactive waste, the intake of underground water from the host rock and the subsequent development of swelling pressure as hydration progresses.[1–12]

Fig. 1(a) shows, in a schematic view, some of the thermo-hydro-mechanical-chemical (THMC) processes involved in the evolution of the barrier during this transient saturation period. The radioactive waste emits heat that is transported through the bentonite to the host rock producing a temperature rise that reduces as the distance to the radioactive waste increases. The temperature rise produces water evaporation in the inner part of the barrier that results in a drying of the bentonite. Vapour migrates towards the outer regions of the barrier where it condenses due to the lower temperature prevailing there. Because the bentonite is unsaturated and, therefore, under suction, water flows from the host rock to the barrier. Consequently, the barrier hydrates, starting in the outer zones close to the host rock and progressively moving inwards. Because of the low permeability of bentonite and host rock, hydration proceeds quite slowly but it is expected that the buffer material will become fully saturated in the long term. Associated with those

* Corresponding author.
E-mail address: sugita.yutaka@jaea.go.jp (Y. Sugita).

https://doi.org/10.1016/j.gete.2025.100668
Received 31 July 2024; Received in revised form 20 March 2025; Accepted 20 March 2025
Available online 29 March 2025

thermo-hydraulic phenomena, there are also mechanical effects: the buffer material deformation due to changes in temperature, suction and stresses and development of the bentonite swelling stress as hydration progresses. In any case, a proper understanding of the processes occurring during the transient period, requires the appropriate simulation of the evolution of the engineered barrier by means of coupled numerical analyses. Fig. 1(b) shows diagram of typical interaction among the coupled THM phenomena considered in the numerical analysis.

In this article we present results from an international modeling comparison study of controlled in-situ, full scale EBS experiment[13,14] that has been conducted at the Horonobe URL, Japan. The study was part of the international collaborative project DECOVALEX-2023 (from 2020 to 2023) where it was denoted Task D.[15] The in-situ, full scale EBS experiment is the Horonobe EBS experiment which has the engineered barrier consists of a simulated overpack and the buffer material, and the experimental gallery is backfilled with the backfill material (Fig. 2). In the Horonobe EBS experiment, the heats generated by an electrical heater represents radioactive decay heat, and a water injection system provides a source of infiltration of groundwater infiltration as shown in Fig. 1a) (details will be described later). This means that the Horonobe EBS experiment does not use actual radioactive waste.

Six modeling teams (research teams) participated in DECOVALEX-2023 Task D, namely: Federal Institute for Geosciences and Natural Resources (BGR), State Key Laboratory of Geomechanics and Geotechnical Engineering, Institute of Rock and Soil Mechanics, Chinese Academy of Sciences (CAS), Japan Atomic Energy Agency (JAEA), Korea Atomic Energy Research Institute (KAERI), Sandia National Laboratory (SNL) and Taiwan Power Company (Taipower) (Sinotech Engineering Consultants, Inc. represented Taipower research team). Task D consisted of roughly two steps, Step 1 simulated the results of laboratory tests and Step 2 simulated the results of the Horonobe EBS experiment. Modeling team identified the parameters for simulation of the Step 2 through simulations of the Step 1. One of the Step 1 which simulated displacement of the specimen (swelling behaviour) supported the Step 2 which simulated interaction between the buffer material and the backfill material. While this article aims at synthesizing some of the most important results and findings related to interpretative modeling of observed thermal-hydro-mechanical behaviour in the buffer material, a complete coverage of all results and comparisons are reported in Sugita et al.[15]

The paper presents a summary account of the work carried out within the Task D and assesses the capabilities of numerical analysis approaches to simulate and interpret the observed TH and THM behaviour of the bentonite barriers, with a particular focus on the heating and cooling conditions. It is structured as follows: for each of the laboratory tests (for the Step 1) and the Horonobe EBS experiment (for the Step 2), the contents are briefly described first, the main features of the comparisons between numerical results and laboratory and field observations are presented and discussed. A concluding remarks section closes the paper.

2. Task D description

Task D consisted of the three steps, a preliminary step (Step 0), simulation of the laboratory tests (Step 1) and simulation of the in-situ full-scale EBS experiment (Step 2). Step 0 is defined as a preparation step. Task D research teams were required to improve their analysis codes to take into account changes in the dry density of the buffer material. Step 1 is the numerical simulation of the measurement results of the laboratory tests. The simulation results of the laboratory test measurement results are evaluated.

Step 1 is divided into 4 sub steps. Schematic illustrations of the experiments are shown in Fig. 3. Step 1–1 is the swelling pressure test.[16] The volume of the specimen is fixed and temperature is constant (room temperature). This sub-step calculates H-M behaviour. Step 1–2 is the free swelling test where the volume (and hence density) of the specimen can change.[16] This sub-step considers H-M behaviour. Step 1–3 is the infiltration test, here the volume of the specimen is fixed. This sub step considers mainly H-M behaviour (specimen volume change is constrained.).[17] Inlet waters are distilled water and NaCl (0.2 mol) water, therefore considering water chemistry (we identified it is “C”) calculations are possible. Step 1–4 is the temperature gradient moisture diffusion test.[18] The volume of the specimen is fixed. This sub step considers T-H behaviour (specimen volume change is constrained.).

In the Step 1–1 (Swelling pressure test) and the Step 1–2 (free swelling test), the specimen was a cylindrical shape with a diameter of 6 cm, and height of 2 cm. Test water was distilled water and injected from the bottom of the specimen, and pressure head of the water was 0 MPa. The test conditions of the Step 1–1 and the Step 1–2 are shown in Tables 1 and 2, respectively.

In the Step 1–2, three loading pressures were selected to restrain the deformation of the specimen, taking into account the swelling pressure of the specimen.

In the Step 1–3 (infiltration test), the specimen was a cylindrical shape with a diameter of 5 cm, and height of 5 cm. Test water was distilled water and injected from the bottom of the specimen, and pressure head of the water was 0 MPa. The test conditions of the Step 1–3 are shown in Table 3. The specimen was divided (cut) into ten pieces after the test, and water content (and hence saturation) was calculated.

In the Step 1–4 (temperature gradient moisture diffusion test), the specimen was a cylindrical shape with a diameter of 5 cm, and height of

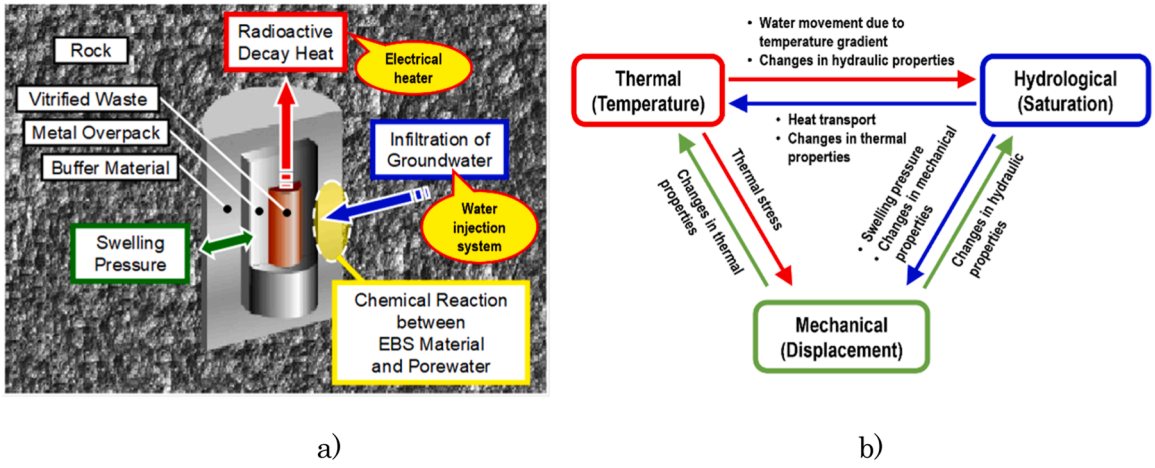

Fig. 1. Coupled THM phenomena: a) schematic view of the coupled THMC phenomena in the near-field (around the EBS), b) diagram of interaction among coupled THM phenomena considered in the numerical analysis.

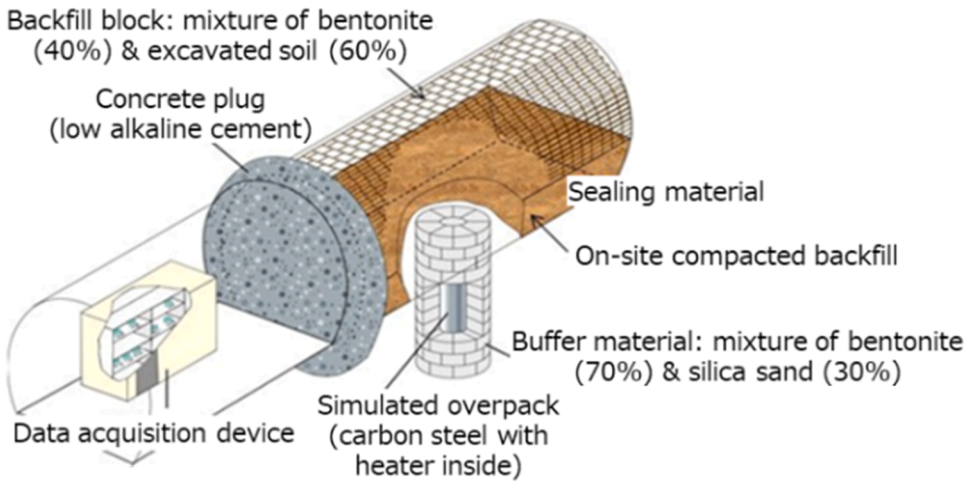

Fig. 2. The Horonobe EBS experiment (Schematic view).

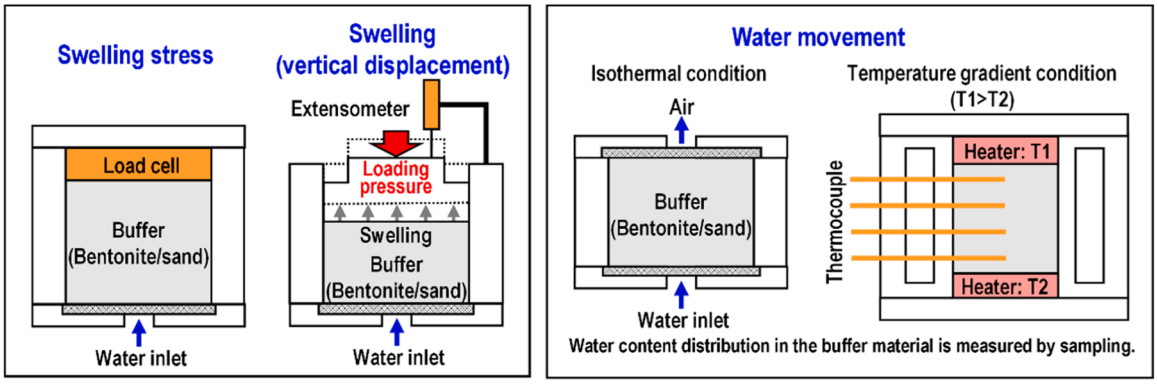

Fig. 3. Schematic view of laboratory tests for the Step 1.

Table 1
Test conditions of the swelling pressure test (Step 1–1).

Case	Dry density	Initial water content	
	(Mg/m^3)	Set value	(wt%)
SP−16-NWC	1.6	Natural water content	7.2
SP−16-SR50		Sr= 50 %	12.9
SP−16-SR80		Sr= 80 %	20.7
SP−18-EBS−1	1.8	Horonobe EBS Experiment	10.5
SP−18-EBS−2			
SP−18-EBS−3			

10 cm. The test specimen was installed into the heat insulation cell. The temperature of both upper and lower sides was controlled by a hot water circulation system. The temperature of the lower side was 70 °C. The upper side was 30 °C. The test conditions of the Step 1–4 are shown in Table 4. The specimen was divided (cut) into ten pieces after the test, and water content (and hence saturation) of each piece calculated.

Table 2
Test conditions of the free swelling test (Step 1–2).

Case	Dry density (Mg/m^3)	Initial water content (wt%)	Loading pressure (kPa)
SD−16–460-SR50	1.6	12.9	460
SD−16–340-SR50			340
SD−16–250-SR50			250
SD−18–1350-SR50	1.8	10.5	1350
SD−18–900-SR50			900
SD−18–450-SR50			450

Table 3
Test conditions of the infiltration test (Step 1–3).

Case	Dry density (Mg/m^3)	Initial water content (wt%)	Test water
IN−18-DW	1.8	8.88	Distilled water
IN−18-GW	1.8	7.36	NaCl 0.2 mol

Step 2 focused on simulation of the coupled THM phenomena as shown in Fig. 1 using in-situ full scale EBS installed in the underground research laboratory (URL) (shown in Fig. 4). The measured data using installed sensors at the selected comparison points of the Horonobe EBS experiment were calculated. Since the Horonobe EBS experiment demonstrates the vertical emplacement option of the EBS, the gallery is also backfilled with the backfill material as shown in Fig. 2. The expecting coupled THM phenomena is complex including interaction between the buffer and backfill materials. Such phenomena include deformation of the buffer and backfill material. This means that the numerical simulations of the Horonobe EBS experiment need to consider interaction

Table 4
Test conditions of the temperature gradient moisture diffusion test (Step 1–4).

Material	Kunigel V1®: 70 wt% Silica sand: 30 wt%
Dry density	1.8 Mg/m^3
Initial water content	10.5 wt%
Temperature	Upper part: 30 °C, 20–25 °C (TG−7–1 and 7–2) Lower part: 70 °C
Test period	7, 11 and 18 days

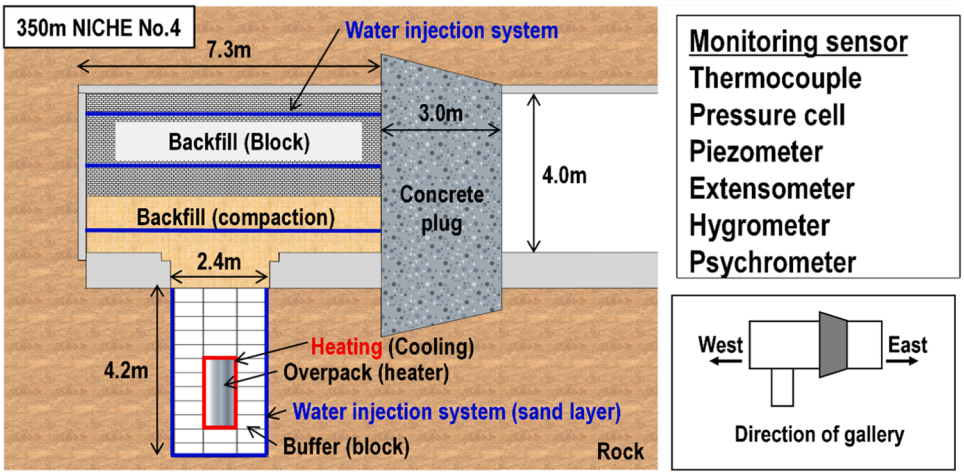

Fig. 4. Schematic view of in situ EBS experiment for the Step 2.

between the buffer material and the backfill material, too. For example, when the saturated and swelling buffer material expand, the density (volume) of the buffer material may change. In Step 2, considering mechanical behaviour in the simulation is important.

On the other hand, concrete support of the gallery (shotcrete and roadbed concrete are described in Fig. 8 in Section 3) is very solid and the displacement of the support is almost limited. This situation may simplify the model for simulation, such as only the simulated EBS and backfill material regions are modeled.

In Step 1, laboratory experiments were modelled numerically in order to understand the processes within the buffer and backfill materials. This Step includes swelling tests (Step 1–1 and 1–2), hydraulic flow tests (Step 1–3) and the temperature gradient moisture diffusion test (Step 1–4). With these simulations, the main parameters of the THM analysis were identified for Step 2 - the simulation of the Horonobe EBS experiment. The research teams validate their own numerical models by comparing calculated results to the measurement data provided by JAEA.

We now discuss some aspects of this task, particularly Step 2. Details of the Horonobe EBS experiment are described in Section 3.

The Horonobe EBS experiment is currently undergoing testing, and verification of whether the values measured by the measurement sensors are correct will be left to the dismantling investigation of the Horonobe EBS experiment that will be carried out in the future. Therefore, the analysis in Step 2 in particular will be a comparative verification under the provisional condition that the values measured by the measurement sensors are correct.

Since the Horonobe EBS experiment is being conducted at the Horonobe URL, where saline groundwater is present, it is expected that the geochemical impact on the physical and hydraulic properties of the buffer material and the backfill material will be verified. However, no sensors have been installed to measure geochemical data. Therefore, consideration of the geochemical impact will depend on the results of the dismantling investigation that will be conducted in the future.

For this reason, Step 2 focused on the temperature, water pressure, saturation, swelling pressure, and displacement, values of which were obtained using the measurement sensors installed in the Horonobe EBS experiment. However, sufficient measurement data has not necessarily been obtained for some of these items.

During the course of Task D, it became clear that the Horonobe EBS Experiment, which was the core of Task D, did not provide enough measurement data to verify the numerical analysis that was initially planned. Threfore, in Step 2, instead of each participating team conducting an analysis under common conditions and comparing the results, the focus was on each participating team taking their own approach and summarizing how that affected the analysis results.

Specifically, this concerns the concept of setting boundary conditions and the concept of the modeling domain for numerical analysis. The Horonobe EBS experiment is conducted at the Horonobe URL, where various tests are conducted simultaneously. Therefore, the underground galleries are open, and groundwater recovery in the surrounding rock cannot be expected, as is the case with geological disposal of radioactive waste. In such a deep URL environment, measures are taken to saturate the rock mass around the EBS by supplying groundwater to the boundary area around the Horonobe EBS experiment. The research team was provided with both the injection pressure and the amount of groundwater to be injected, allowing them to determine how to set the boundary conditions.

In the Horonobe EBS experiment, the heat generation phenomenon from radioactive waste was simulated by an electrical heater system built into the simulated ovepack. The temperature conditions of the Horonobe EBS experiment are controlled by the surface temperature of the simulated overpack. Here, both the heat power of the electric heater and the surface temperature of the simulated overpack were monitored. The research team was provided with both the heat power of the electrical heater and the surface temperature of the simulated ovepack, allowing them to determine how to set the boundary conditions.

The mechanical stability of the galleries at the Horonobe URL is basically maintained by concrete supports, which are considered to prevent earth pressure from the host rock from acting directly on the EBS during experiment period. No concrete supports are installed in the test pit where the EBS is installed, but it is considered that the stress state around the gallery is redistributed during the gallery excavation, reducing the stress acting on the test pit. The research team had chance to decide the modeling domain, such as considering just EBS region (host rock is not considered), consideling the EBS and host rock around the EBS.

The domain that the research team modeled for their analysis and the boundary conditions they selected are described later in Section 5.

3. Horonobe EBS experiment

The Horonobe EBS experiment has been performed at the 350 m depth gallery in the Horonobe URL as show in Fig. 5. The full-scale EBS performance experiment performed in the 350 m gallery of the Horonobe Underground Research Laboratory in Japan is a mock-up of the EBS described in the second progress report on research and development for the geological disposal of high-level radioactive waste (HLW) in Japan.[2] Since the galleries of the URL are still open to perform various R&D programs there, groundwater pressure in the rock mass around the galleries is low. Therefore, water injection systems were installed in the test pit (where the EBS is installed) and the gallery to create hydraulic

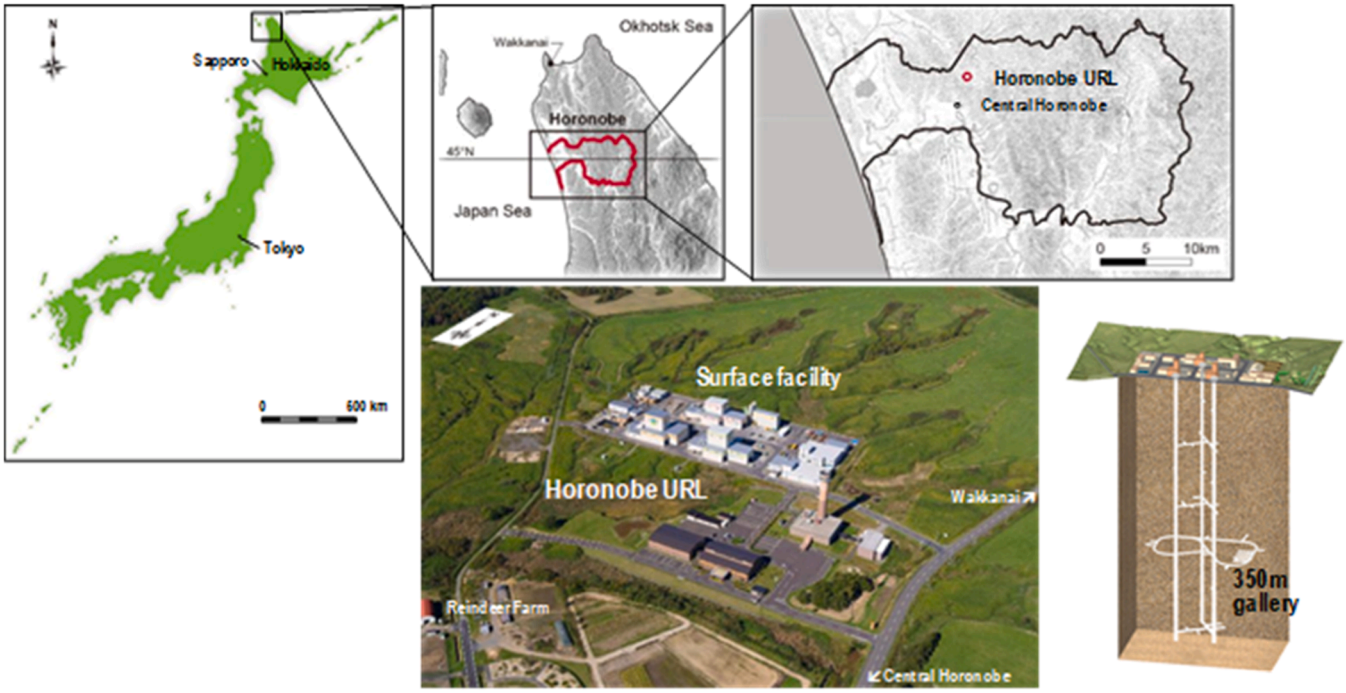

Fig. 5. The Horonobe URL.

boundary conditions as shown in Fig. 6. These developed experimental conditions were important information to simulate the coupled THM behaviour in the EBS, especially the buffer material and the backfill material, in Step 2.

In the Japanese EBS concept, the HLW consists of vitrified waste encapsulated in carbon steel overpacks (i.e. canisters). In the Horonobe EBS experiment, the buffer material, a mixture of the Japanese bentonite (Kunigel® V1) and sand compacted to high density, was installed into the test pit. The simulated overpack was enclosed by the buffer material. Since the Horonobe EBS experiment demonstrates the vertical emplacement option of the EBS, the experimental gallery just above the EBS is backfilled. The backfill material is a mixture of the Kunigel® V1 bentonite and crushed rock (siliceous clay).

In the Horonobe EBS experiment, the scale, dimensions and shape of the EBS and experimental gallery were defined according to the H12 concept.[2] Heat generation of the waste was simulated by using a heater system installed in the simulated overpack. The temperature at the surface of the simulated overpack was controlled to be below 100 °C to avoid chemical alteration of the buffer material. The backfilled experimental gallery for the Horonobe EBS experiment was isolated by a concrete plug from the opened gallery.[13,14]

3.1. Test conditions of Horonobe EBS experiment

Fig. 7 shows EBS condition in the test pit. The diameter of the test pit is 2400 mm. The diameter of the buffer material (eight block pieces forming an annulus shape around the canister) is 2260 mm. Height of the buffer material is 4200 mm. There are 12 layers of the buffer material blocks. The buffer material is mixture of bentonite (Kunigel® V1) and silica sand. Silica sand is the mixture of two kinds of silica sand (No.3 and No.5). The dry density of the buffer material (block) is 1.8 Mg/m^3. The dry density of the buffer material (powder), which filles the gap between the buffer material and the simulated overpack, is 1.2 Mg/m^3. Silica sand fills the gap between the buffer material blocks and rock mass.

Fig. 8 shows backfilling condition in the test gallery. Two backfilling techniques were applied. The lower part was backfilled using direct compaction method. The upper part was backfilled using block installation method. The backfill material is the mixture of bentonite and excavated soil. Bentonite is Kunigel® V1. Dry density of the backfill material are 1.2 Mg/m^3 (compaction) and 1.4 Mg/m^3 (block).

In the Horonobe EBS experiment, thermal and hydraulic conditions are developed using an electrical heater system and water injection system respectively. The electrical heater system is installed in the simulated overpack (820 mm in diameter and 1730 mm in height). The electrical heater system was designed considering the size (height) of the simulated overpack and required power. This heater system has two heaters (heater ch. 1 and ch. 2) as shown in Fig. 9. Capacities of the heater are 4330 W (heater ch.1) and 8670 W (heater ch.2). Running heater power (W) is monitored. In the simulated overpack, the weights are installed to demonstrate weight of the reference overpack in Japan. The space in the simulated overpack is filled with oil. Fig. 10 shows layout of the thermocouple sensors in sand layer in the test pit and on surface of the simulated overpack.

Fig. 11 shows relationship between elapsed time and temperature as monitored by thermocouple sensors bolted to the surface of the simulated overpack. The heating phase lasted around 2000 days, and cooling phase lasted around 700 days. The cooling phase is divided into two subphases. The target temperature for cooling phase 1 is about 50 °C, and for cooling phase 2 about 23 °C (the heaters were turned off before entering cooling phase 2). Monitored temperature has some noise.

Fig. 12 shows relationship between elapsed time and heater power. Heater ch.2 did not work well. It stopped working only 10 days after the start of heating phase. Only heater ch.1 has worked to keep temperature for heating phase and cooling phase 1. After 1200 days, the variation in heater power had increased, and this influence can also be seen from the temperature measurements as shown in Fig. 11.

The control equipment of the groundwater injection system as shown in Fig. 6 are located outside of the concrete plug and includes a flow meter and pressure gauge. Therefore, both injection water volume and injection water pressure are monitored.

One new borehole was drilled to obtain groundwater for injection. This borehole is isolated by a packer system. This borehole and the water injection system are directly connected by a tube, therefore, groundwater is injected into the test pit and experiment gallery by the water injection system without any exposure to air. The water injection

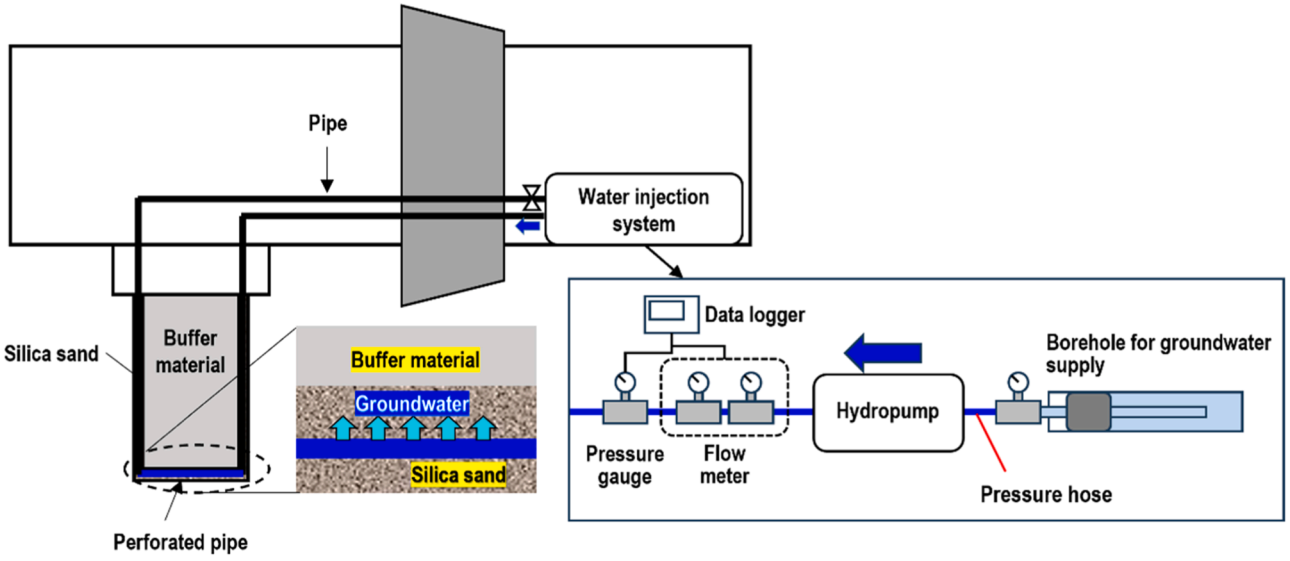

a)

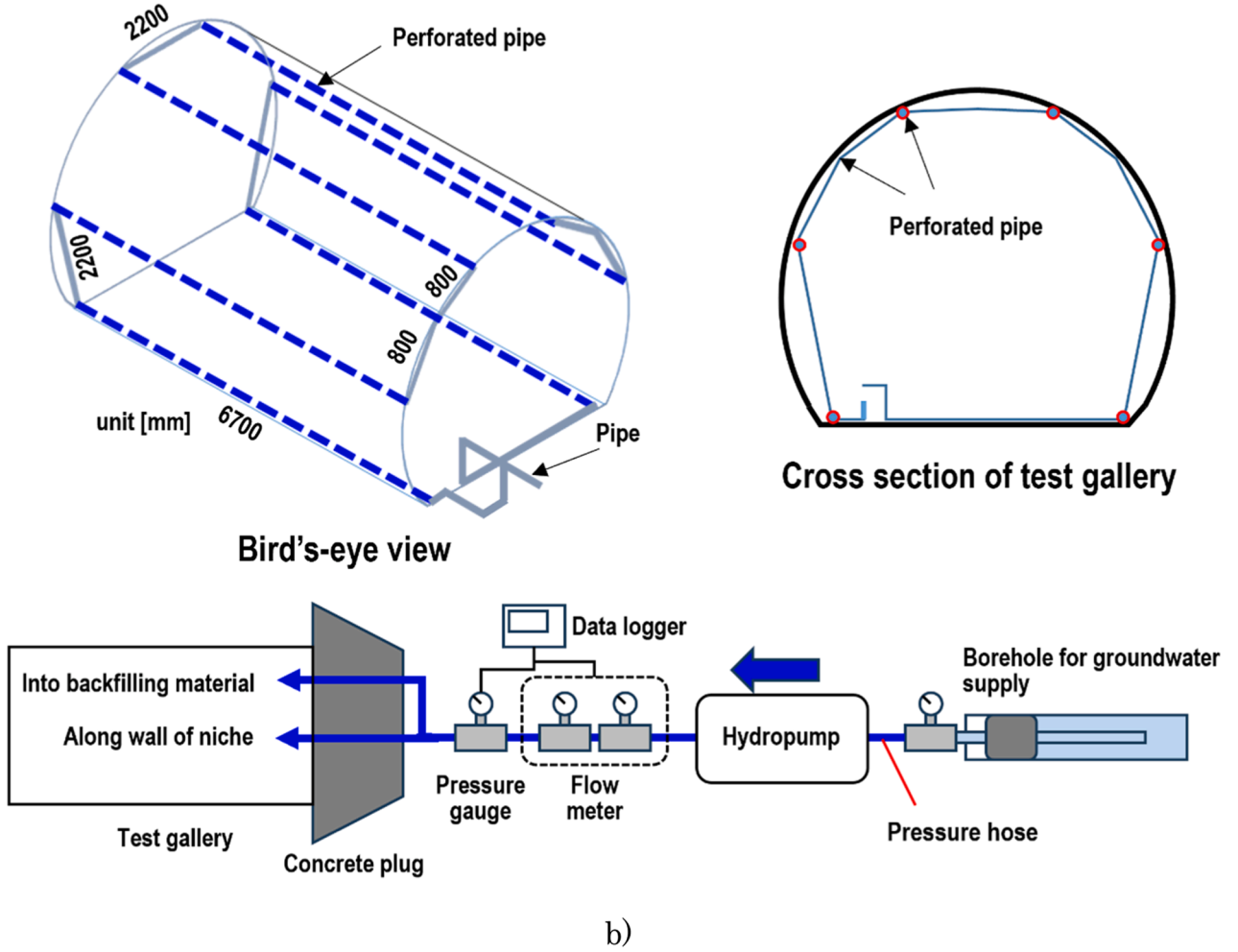

b)

Fig. 6. Water injection system: a) test pit; b) test gallery.

Materials	Bentonite (Kunigel V1®)
	Silica sand
Mixing rate	Kunigel V1® 70 wt% Silica sand 30 wt% (No.3:No.5= 15 wt%:15 wt%)
Water content	10.5 wt%
Dry density	Block 1.8 Mg/m^3 Powder 1.2 Mg/m^3

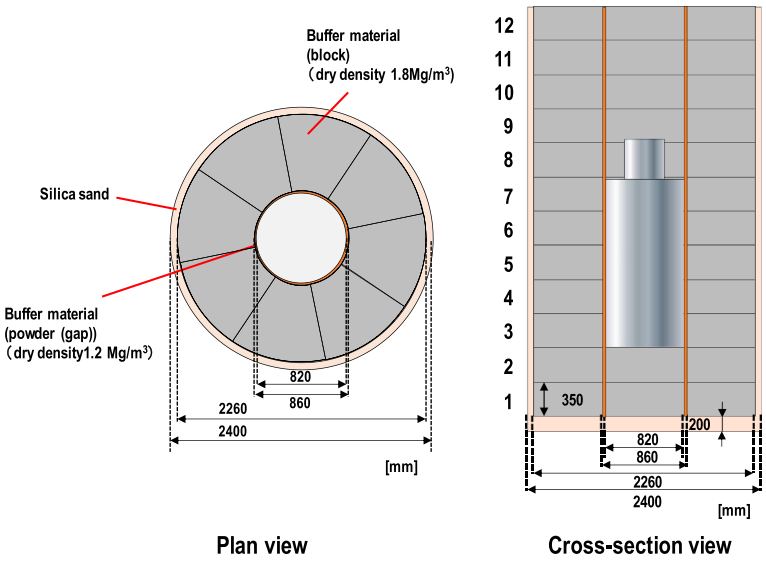

Fig. 7. EBS condition in the test pit.

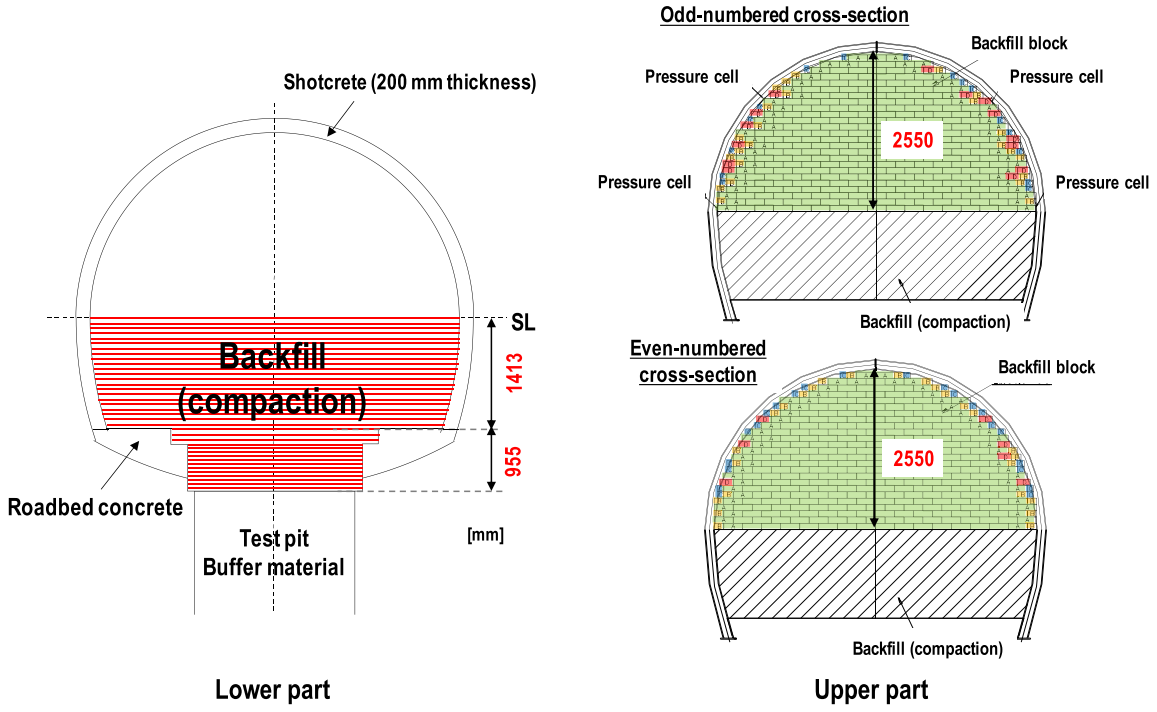

Fig. 8. Backfilling condition in the test gallery.

pressure was controlled by a pump built into the water injection system. Depending on the amount of groundwater supplied, water injection was not continuous but intermittent, which resulted in spikes in the monitored water injection pressure data (Fig. 13). This is also due to the large fluctuations in the monitored injection water volume (flow rate) (Fig. 14).

4. Parameters

In this section, parameters of the materials required for the simulation of Task D presented by JAEA are summarized. Tables 5–8 summarize the parameters of the Horonobe EBS experiment. The materials listed are silica sand (gap filling material), concrete (plug), backfill material (compaction and block), buffer material, simulated overpack and oil (inside simulated overpack).

Young's modulus (elastic modulus E50) of the buffer material is defined by Eq-1 based on laboratory test results shown in Fig. 15.[16]

$$E_{50} = A(S_r - 100) + B \tag{1}$$

$$A = 0.00006e^{6.635\rho_d}$$

$$B = 7.576\rho_d - 6.8387$$

Here, E_{50} is Elastic modulus E50. S_r is saturation. ρ_d is dry density.

Thermal conductivity is defined by Eq-2 using parameters in Table 9.[16]

$$\lambda = A + B\omega + C\omega^2 + D\rho_d \tag{2}$$

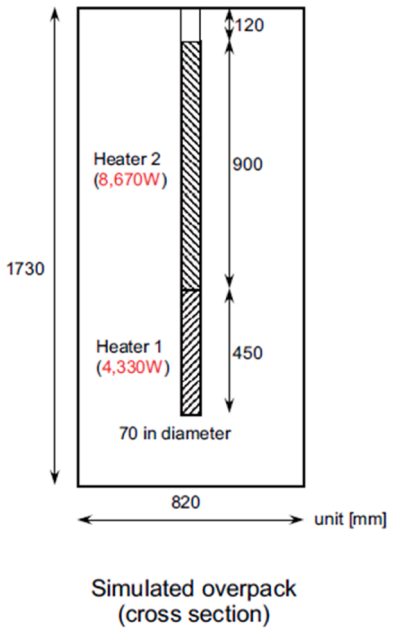

Fig. 9. Electrical heater system.

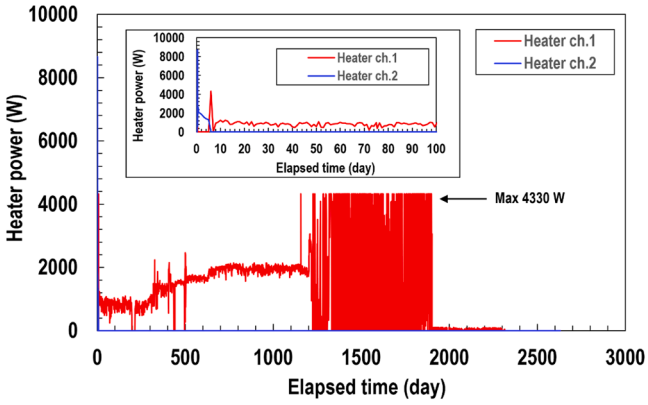

Fig. 12. Relationship between heater powers and elapsed time.

Here, λ is thermal conductivity. ω is water content. ρ_d is dry density. Especially, thermal conductivity of the buffer material (dry density is 1.8 Mg/m^3) is shown in Table 10.

Specific heat is defined by Eq-3 using parameters in Table 11.[16]

$$C = \frac{p_2 + p_3\omega}{p_1 + \omega} \tag{3}$$

Here, C is specific heat (kJ/kg K). ω is water content (wt%).

Intrinsic permeability κ is defined by Eq-4 using parameters in

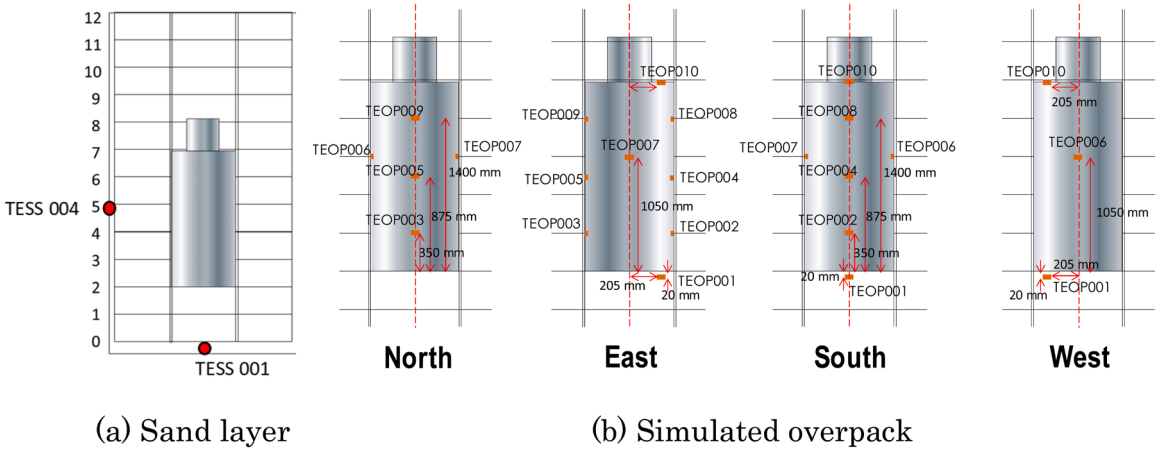

Fig. 10. Layout of thermocouple sensors (a) in sand layer; (b) on surface of the simulated overpack.

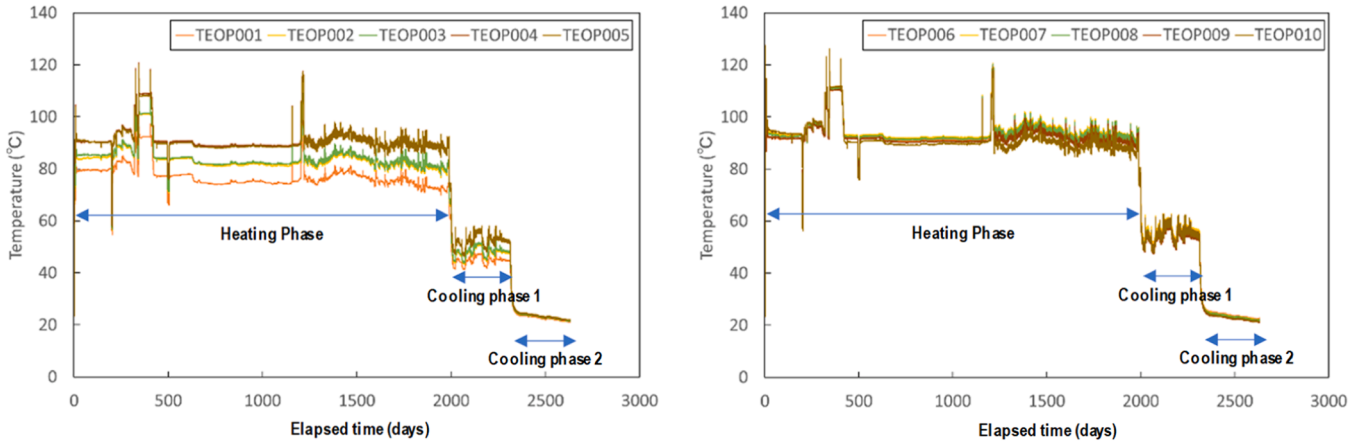

Fig. 11. Relationship between elapsed time and temperature monitored by thermocouple sensors on surface of the simulated overpack.

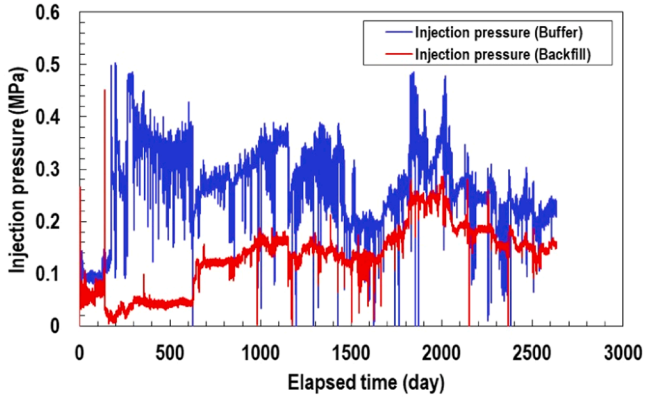

Fig. 13. Relationship between injection pressure and elapsed time.

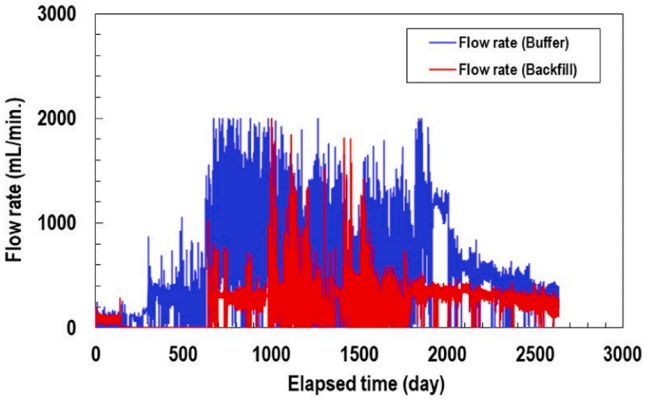

Fig. 14. Relationship between flow rate and elapsed time.

Table 5
Parameters of the Horonobe EBS experiment (buffer material).

Parameter	Unit	Buffer material (block)		Buffer material (gap)	
		1.8		1.2	
Soil particle density	Mg/m^3	2.68		2.68	
Dry density	Mg/m^3	1.8		1.2	
Porosity	-	0.328		0.552	
Young's modulus	MPa	Eq−1		Eq−1	
Poisson's ratio	-	0.3		0.3	
Thermal linear expansion coefficient	1/K	1.00×10^{-6}		1.00×10^{-6}	
Initial saturation	-	0.58		0.228	
Thermal conductivity	W/m K	Eq−2		Eq−2	
Specific heat	kJ/kg K	Eq−3		Eq−3	
Intrinsic permeability	m^2	DI water Eq−4	Horonobe GW Eq−4	DI water Eq−4	Horonobe GW Eq−4
Water retention curve	-	Eq−8		Eq−8	
Specific permeability	-	Eq−5		Eq−5	
Maximum swelling pressure	MPa	DI water Eq−6	Horonobe GW Eq−7	DI water Eq−6	Horonobe GW Eq−7

Table 6
Parameters of the Horonobe EBS experiment (backfill material).

Parameter	Unit	Backfill material	
		Compaction	Block
Soil particle density	Mg/m^3	2.593	2.593
Dry density	Mg/m^3	1.2	1.4
Porosity	-	0.538	0.46
Young's modulus	MPa	3.92	17.95
Poisson's ratio	-	0.4	0.4
Thermal linear expansion coefficient	1/K	1.00×10^{-6}	1.00×10^{-6}
Initial saturation	-	0.91	0.91
Thermal conductivity	W/m K	Eq−2	Eq−2
Specific heat	kJ/kg K	Eq−3	Eq−3
Intrinsic permeability	m^2	3.00×10^{-18}	1.76×10^{-19}
Water retention curve	-	Eq−8	Eq−8
Specific permeability	-	Eq−9	Eq−9
Maximum swelling pressure	MPa	0.1	1.0

Table 7
Parameters of the Horonobe EBS experiment (host rock, sand layer and concrete).

Parameter	Unit	Host rock	Silica sand	Concrete
Soil particle density	Mg/m^3	2.45	2.51	2.62
Dry density	Mg/m^3	1.42	1.4	2.28
Porosity	-	0.416	0.442	0.13
Young's modulus	MPa	1820	1820-	2.94×10^4
Poisson's ratio	-	0.17	0.3	0.2
Thermal linear expansion coefficient	1/K	1.33×10^{-5}	1.33×10^{-5}	1.00×10^{-5}
Initial saturation	-	-	1	1
Thermal conductivity	W/m K	Eq−2	2.04	2.56
Specific heat	kJ/kg K	Eq−3	1.28	1.05
Intrinsic permeability	m^2	7.5×10^{-18}	1.00×10^{-13}	9.10×10^{-18}
Water retention curve	-	Eq−8	-	-
Specific permeability	-	Eq−9	-	-

Table 8
Parameters of the Horonobe EBS experiment (simulated overpack).

Parameter	Unit	Simulated overpack
Density	Mg/m^3	7.8
Young's modulus	MPa	2.00×10^5
Poisson's ratio	-	0.2
Thermal linear expansion coefficient	1/K	1.64×10^{-6}
Initial saturation	-	0.5
Thermal conductivity	W/m K	53
Specific heat	kJ/kg K	0.46

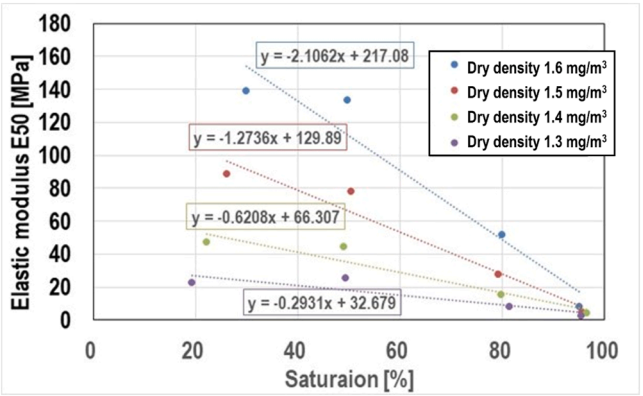

Fig. 15. Relationship between elastic modulus E50 and saturation (buffer material).[16]

Table 9
Thermal conductivity parameters.

	A	B	C	D	Dry (W/m K)	Saturated (W/m K)
Buffer material	−2.01	7.56E−02	−7.00E−14	1.56	0.58	1.23
Rock mass	5.79E−01	1.97E−02	0	0	0.80	1.94
Backfill material (Compaction)	2.24E−01	2.13E−02	0	0	0.22	1.17
Backfill material (Block)	3.39E−01	2.97E−02	0	0	0.34	1.31

Table 10
Thermal conductivity (buffer material).

Dry density (Mg/m^3)	Thermal conductivity (dry) (W/m K)	Thermal conductivity (saturated) (W/m K)
1.8	7.98E−01	1.94

Table 11
Specific heat parameters.

	p_1	p_2	p_3
Buffer material	100	67.3	4.18
Rock mass	100	62.6	3.20
Backfill material	100	40.0	4.18

Table 12
Intrinsic permeability parameters (1/2).

ρ_s	2.68
R_s	30

Tables 12 and 13.[19–21]

$$\kappa = \exp(a + b\rho_b + c\rho_b^2) \tag{4}$$

$$\rho_b = \frac{\rho_d(100 - R_s)}{100 - \left(\frac{\rho_d R_s}{\rho_s}\right)}$$

Here, ρ_b is effective clay density. ρ_d is dry density. R_s is mixing ratio of sand. ρ_s is soil particle density of sand.

Specific permeability k_r is defined by Eq-5.[16]

$$k_r = S_r^3 \tag{5}$$

Here, S_r is saturation.

Maximum swelling pressure is defined by Eq-6 (DI water), Eq-7 (Horonobe groundwater) using parameters in Table 14 and Fig. 16.[21]

$$\sigma = \exp\left(3.94\rho_b^3 - 13.71\rho_b^2 + 18.06\rho_b - 9.60\right) \tag{6}$$

$: [0.50 \leqq \rho_b \leqq 2.00]$

$$\sigma = \exp\left(4.24\rho_b^3 - 20.04\rho_b^2 + 37.63\rho_b - 26.07\right) \tag{7}$$

$: [1.17 \leqq \rho_b \leqq 1.80]$

$$\rho_b = \frac{\rho_d(100 - R_s)}{100 - \left(\frac{\rho_d R_s}{\rho_s}\right)}$$

Here, ρ_b is effective clay density. ρ_d is dry density. R_s is mixing ratio of sand. ρ_s is soil particle density of sand.

Van Genuchten model[22] parameters are defined by Eq-8 and Eq-9 using parameters in Table 15.

$$S_e = \frac{\theta - \theta_r}{\theta_s - \theta} = [1 + |\alpha\Psi|^n]^{-m} \tag{8}$$

$$m = 1 - \frac{1}{n}$$

Table 13
Intrinsic permeability parameters (2/2).

	a	b	c
DW	−42.1	1.1447	−2.1232
Groundwater (Horonobe)	−41.466	4.316	−4.069
Salt water	−47.155	15.138	−7.878

Table 14
Maximum swelling pressure parameters.

ρ_s	2.68
R_s	30

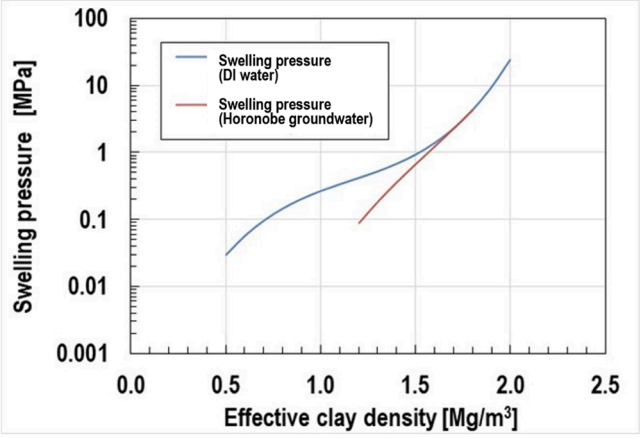

Fig. 16. Relationship between swelling pressure and effective clay density.[19]

$$k_r = \sqrt{S_r}\left[1 - (1 - S_e^{1/n})^n\right]^2 \tag{9}$$

Here, S_e is effective saturation. θ is volumetric water content, θ_r is saturated volumetric water content, θ_r is residual volumetric water content, Ψ is suction (mH_2O), α and n are the fitting parameters. k_r is Specific permeability and S_r is saturation.

5. Approaches of research teams

Table 16 shows the approaches of the research teams. BGR team uses OpenGeoSys,[23] CAS team uses CASRock,[24,25] JAEA team uses THAMES[26] and MACBECE,[27] KAERI team uses COMSOL,[28] SNL team uses PFLOTRAN[29] and the Taipower team uses COMSOL,[30] respectively.

Table 15
van Genuchten model parameters.

	n	α	θ_s	θ_r
Buffer material (1.2)	1.41	5.10E−02	0.403	0
Buffer material (1.8)	1.38	5.00E−03	0.328	0
Backfill material (1.2)	1.78	5.00E−03	0.538	0
Backfill material (1.4)	1.41	1.70E−03	0.459	0
Host rock	2.01	9.93E−03	0.386	0

The codes used were either directly developed or improved by the research teams. All groups chose a continuum theory approach for modelling the THM processes. The mechanical behaviour of the solid phase was modelled either elastically or elasto-plastically. The fluid phases were calculated either simplified via the Richards equation[31] or as true two-phase flow. All research teams selected continuous media.

Details of the analysis codes used by the research teams can be found in the references cited here, but the key points relevant to this task were highlighted.

Tables 17–22 presents the characteristics of the analytical codes of the reaearsh teams, respectively.

And, the setting of parameters and boundary conditions for Step 2 of the research teams is presented in Tables 23–28, respectively.

6. Results of Step 1

Fig. 17 shows the presented images of the benchmark from Step 1–1 to Step 1–4. Based on these images, Research team considered developing their own model for simulation.

As an example of the simulation results, Fig. 18 shows comparisons of teams' modelling results of Step 1–1. Fig. 18 (a) and (b) show natural water content and Sr= 80 %, respectively.

Regarding the analysis of the laboratory test conditions with the natural water content, the BGR, CAS, JAEA, KAERI and Taipower teams performed the analysis. The process of increasing swelling pressure varied among research teams, but the final swelling pressure was in good agreement with the laboratory test result for all research teams. JAEA (MACBECE) team simulated increasing then decreasing of swelling pressure early in the test well.

Regarding the analysis of the laboratory test condition of Sr= 80 %, BGR, CAS, JAEA and Taipower teams performed the analysis. The form of increasing swelling pressure varied among research teams, but the final swelling pressure was in good agreement with the laboratory test result for JAEA (THAMES) and Taipower teams. The simulated final swelling pressure of BGR, CAS and JAEA (MACBECE) teams were smaller than the laboratory test results.

As an example of the simulation results, Fig. 19 shows comparisons of teams' modelling results of Step 1–2.

Fig. 19 shows displacement evolution with a dry density of 1.6 Mg/m^3. Fig. 19 (a), and (b) show 460 kPa and 250 kPa of loading pressure, respectively. The BGR, CAS, JAEA, KAERI and Taipower teams performed the analysis.

Regarding the analysis of the loading pressure at 460 kPa: this pressure is the largest pressure in the laboratory test conditions. Both the process of increasing displacement and the final displacement were in good agreement with the laboratory test result for BGR, CAS, JAEA (THAMES), KAERI and Taipower teams. JAEA (MACBECE) showed small displacement.

Regarding the analysis of the loading pressure is 250 kPa that this pressure is the smallest pressure in the laboratory test conditions, the KAERI team result is in good agreement with the laboratory test result.

Table 17
Characteristics of analytical code (BGR team).

Team	Characteristics of analytical code
BGR	The finite element method (FEM). All experiments of Step 1 and Step 2 were simulated in a 2D axisymmetric framework with Taylor-Hood-Elements. For bentonite material, a modified Cam-Clay model according to[32] was employed. Here only a small-strain version with constant elastic constants was implemented in OpenGeoSys. The strain was splitted into elastic and plastic components. The inelastic deformations are described by a Modified Cam Clay model,[32] which currently does not consider saturation. The water retention behavior is specified to follow the van Genuchten model[22] driven by the capillary pressure. The porosity permeability relationship in OpenGeoSys is defined as the permeability is assumed to be isotropic. The transport porosity accounts for the mechanical part of the porosity evolution excluding swelling strains. The expression for swelling strain is derived from a simple saturation-dependent power law. The current model for swelling is purely dependent on saturation and lacks an association with porosity evolution, which significantly limits its ability to simulate the swelling of nearly fully saturated materials.

Table 18
Characteristics of analytical code (CAS team).

Team	Characteristics of analytical code
CAS	A combination of the cellular automaton (CA) and the finite element method (FEM). The CA updating rule for solution of physical variables, such as displacement, temperature and fluid flow, on the spatial scale is developed using local equilibrium conditions, in which the local stiffness is from the element stiffness of FEM.[24,25] In Step 1, 2D model was created. In Step2, the dimension of the 3D model was created. The model is discretized into a system composed of hexahedral elements. Non-isothermal, unsaturated fluid flow and mechanical processes are sequentially coupled.[52] The buffer material is viewed as a partially saturated medium considering Richards' equation[31] with vapor added. The water retention curve is described by the van Genuchten model.[22] The water vapor flow is assumed to be driven solely by the thermal gradient. The thermal vapor diffusion coefficient is an empirical function of saturation. The material is assumed to be elastic. The displacement of the buffer material was simulated using a linear elastic mechanical model. The swelling stress path is controlled by a function dependent on the initial saturation.

Other research team results are smaller than the laboratory test result.

This case presented the following tendency. When loading pressure is large, this mean displacement is constrained, the simulation results performed by research teams closely reproduced the laboratory test results. However, as the loading pressure becomes smaller (displacement becomes larger), the simulation results performed by research teams began to vary and do not reproduce the laboratory test results

Table 16
Analytical code and modelling approach.

Research Team		BGR	CAS	JAEA	KAERI	SNL	Taipower
Geometry	Step 1	2-D axisymmetric/ 3-D	3-D	3-D	2-D/3-D	1-D/2-D	2-D/3-D
	Step 2	2-D axisymmetric /3-D	3-D	2-D/3 D	2-D/3-D	1-D/2-D	2-D/3-D
Code		OpenGeoSys	CASRock	THAMES MACBECE	COMSOL	PFLOTRAN	COMSOL
Coupling	Step 1	THM	THM	THM	THM	TH	THM
	Step 2	THM	THM	THM	TH	TH	THM
Mechanical (Buffer)	Step 1	Elasto-plastic	Elastic	Elastic Elasto-plastic	Elasto-plastic	-	Elastic
	Step 2	Elasto-plastic	Elastic	Elastic Elasto-plastic	-	-	Elastic
Hydraulic (phase)		Single phase	Single phase	Single phases	Two phases	Two phases	Single phase

Table 19
Characteristics of analytical code (JAEA team).

Team	Characteristics of analytical code
JAEA	The finite element method (FEM). Simulation using THAMES[26] was 3D model and MACBECE[27] was 2D axisymmetric model. THAMES[26] THAMES is a finite element code for the analysis of coupled thermal, hydraulic and mechanical behaviour of a saturated-unsaturated medium, and has been extended to take into account of the behaviours in the buffer materials such as the water movement due to thermal gradients and swelling phenomena. Regarding governing equations, the constitutive equations differ for each material and saturated and unsaturated conditions.[33,34] The equilibrium equation has to take the swelling behaviour into account. The material is assumed to be elastic. THAMES has problem in simulating deformation behavior. For small deformations, the measured values can be reproduced to some extent, however for larger deformations, the measured values cannot be simulated well. The water retention curve is described by van Genuchten model.[22] The temperature-gradient moisture-diffusion coefficient conformed to the model of Börgesson and Hernelind (1999).[35,36] The parameters of the thermal vapor flow diffusivity assumed two cases. Case 1 is a fitted parameter based on the predicted simulation results of TOUGH2 from another test,[36] while Case 2 is a calibrated parameter based on the test results of Step 1–4. The simulation results of Case 2 show good agreement between the test and simulation results in Step 1–4. MACBECE[27] The unsaturated elasto-plastic constitutive model[34,37] in which the effective degree of saturation is used as a hardening/softening parameter[37,38] was applied to the bentonite material. This model is a simple extension of the Modified Cam-clay model[32] to unsaturated conditions with the addition of relatively few parameters. The yield function of the unsaturated elasto-plastic constitutive model[34,37] is the same as that of the Modified Cam-clay model.[32] The changes over time in the saturation distribution in the buffer material required for the mechanical simulation of MACBECE are obtained from coupled TH simulation results by THAMES. Deformation of the buffer material induces changes in dry density, which also affects thermal and hydraulic properties, but this simulation using MACBECE does not consider changes in thermal and hydraulic properties due to changes in dry density. The simulation of Step 1–1 captured the process of increasing swelling pressure over time, reproducing the tendency for swelling pressure to increase with dry density. The simulation of Step 1–2 captured the behavior of buffer material swelling over time, reproducing the tendency for greater swelling displacement with greater loading pressure and greater drying density.

Table 20
Characteristics of analytical code (KAERI team).

Team	Characteristics of analytical code
KAERI	The finite element method (FEM) For modeling of Step 2 (a representative engineered barrier system situated underground), a 3D model consisting of 711,041 mesh elements was developed. However, due to the extensive computational time ranging from 15 to 24 hours, a 2D axis-symmetric finite element model with 14,186 mesh elements was also utilized, requiring only 30 minutes of computational time. For the THM-coupled analysis, a heat balance equation, two mass balance equations, and a momentum balance equation were used. The water retention curve is described by van Genuchten model.[22] A two-phase flow model, which considers the mass conservation of liquid and gas, was used in the governing equations.[39] Suction was added as an independent variable to consider the influence of saturation, and the plastic yield surface was written in a three-dimensional (3D) stress space. The mechanical performance of the partially saturated buffer material was interpreted using the Barcelona basic model (BBM).[40,41] BBM, which is an extension of the modified Cam clay model (MCCM),[42] is widely used as an elastoplastic model for partially saturated soils.[40,41]

Table 21
Characteristics of analytical code (SNL team).

Team	Characteristics of analytical code
SNL	The finite volume method (FVM) 1-D simulation in Step 1. 2-D multiphase thermos-hydrological (TH) simulations in Step 2. In Step 1–3 and 1–4, the bentonite block was divided into two regions and five having different isotropic permeabilities, respectively. Because it is reasonable to implement heterogeneous permeability regions in the bentonite column and treat this as an input variable constrained by fits of the experimental data.[43,44] For example, many simulations were conducted using the DAKOTA optimization code[45] to evaluate permeabilities of the five zones, initial saturation, and porosities (top and bottom zone only) in Step 1–4. The 2-D model uses PFLOTRAN's GENERAL mode for thermal and hydrologic calculations of two-phase (liquid/gas) flow in porous media. Reducing the dimensionality of the problem also reduces the computational burden of this highly complex system, particularly when considering two-phase flow. This imposes limitations on the representation of some effects and predicted behaviors of coupled processes in porous flow relative to a full 3-D model. Thermal and hydraulic calculations of two-phase (liquid/gas) flow but no reactive transport (i.e., no chemical interactions) or mechanical changes (clay swelling) were considered in these simulations. Reactive transport and chemical interactions were not considered in this model.

Table 22
Characteristics of analytical code (Taipower team).

Team	Characteristics of analytical code
Taipower	The finite element method (FEM) 2D models were created for Step 1. In Step 2, a full 3D simulation was performed. Richards' equation[31] models flow in variably saturated porous media. The form that COMSOL Multiphysics solves is very general and allows for time-dependent changes in both saturated and unsaturated conditions.[22,46] For a linear elastic material, Hooke's law relates the stress tensor to the elastic strain tensor. Hygroscopic swelling is an internal strain caused by changes in moisture content.[47] The heat transfer equation for porous media is derived from the mixture rule on energies appearing in solid and fluid heat transfer equations.[48] They used thermal and transport model to solve the TH coupling problem. COMSOL cannot be calculated when the boundaries are all no-flux and saturation cannot change with temperature in the current formulation. Taipower team used Antoine's equation[49] to model water vapour migration. To simulate the behavior of water movement due to heat, it is necessary to calculate the relationship between temperature and vapor diffusion. The water retention curve is described by the van Genuchten model.[22] A transport model was used to simulate the diffusion behavior of water vapor. The relationship between water vapor and temperature was calculated in conjunction with the Antoine equation, and the affected part iterated fed back to the Richard equation[31] in source term. A maximum swelling pressure is required to calculate the coefficient of hygroscopic swelling β_h. Hygroscopic swelling is an internal strain caused by changes in moisture content.[50] The experimental data is applied to estimate the β_h parameter.

well. The mechanical parameter (Young's modulus) identified by fundamental laboratory tests predicted a small displacement when using an elastic-only approach. Although the elastic model approach was selected, adding equations for considering swelling displacement can improve the simulation results.

As an example of the simulation results, Fig. 20 shows comparisons of teams' modelling results of Step 1–3.

Fig. 20 shows saturation distributions of ground water (GW). Fig. 20 (a) and (b) show 1 day and 30 days, respectively. The CAS, JAEA, KAERI, SNL and Taipower teams performed the analysis. The SNL team performed two simulations using homogenous media and heterogenous media to model the specimens. In the heterogeneous medium model, the

Table 23
Parameters and boundary conditions for Step 2 (BGR team).

Team	Parameters and boundary conditions for Step 2
BGR	[Parameters for Step 2] In Step 2 the simulations modeled host rock, simulated overpack, buffer material, sand layer in the test pit, backfill block, backfill compact, concrete support, and gallery. For the buffer the material parameters founded in Step 1 were used. With two experiments (Step 1–1 and 1–2), the slope of the critical state line, the difference of the slopes, the initial pre-consolidation pressure and the swelling stress parameter of the buffer material were identified. In Step1–3 the permeability related parameters of the buffer material are identified, namely the intrinsic permeability and the exponent of the porosity dependent permeability function.[51] In Step 1–4, by a parameter variation, the tortuosity factor and the diffusion enhancement factor are determined. The backfill materials were only slightly modified from this parameter setting. For all other parameters the given values were used in the simulation. [Boundary conditions for Step 2] Originally, there were two heater channels active, but one of them had a defect within the first days of the experiment. Since the signal is quite noisy, a piecewise linear (PL) approximation was computed as heat source. It was constructed in a way, such that the generated heat (integral of the power) has only a minor error. This energy can be incorporated as a volumetric heat source within the computational model. Regrettably, this approach results in excessively elevated temperatures at the sensor locations. The average value of two measured temperature (the highest and the lowest on the surface of the simulated overpack) were applied to thermal boundary condition. The resulting pore pressure at the sensor points is far too high by applying the flow directly. Therefore, the measured pore pressure of the sensor points was prescribed in the simulation as the hydraulic boundary condition. Boundary conditions for the heating element and water injection were defined using measured data as Dirichlet boundaries.

Table 24
Parameters and boundary conditions for Step 2 (CAS team).

Team	Parameters and boundary conditions for Step 2
CAS	[Parameters for Step 2] In Step 2 the simulations modeled rock mass, simulated overpack, buffer material, sand layer in the test pit, backfill block, backfill compact, concrete (plug and support) and gallery. The buffer material is viewed as a partially saturated medium. By considering Richards' equation[31] with vapour added. In Step1–4, some of the parameters are from Step1–3. Regarding vapor diffusion coefficient, different tortuosity in vapor diffusion coefficient is considered to study its influence on the results. The initial water content is 10.5 wt%. When tortuosity is 0.5, the modeling data is more consistent with experimental data. For all other parameters the given values were used in the simulation. [Boundary conditions for Step 2] Applied boundary conditions were the temperature of the surface of the simulated overpack (thermal) and measured groundwater pressure in the sand layer in the test pit and the backfill material (hydraulic). These input data were simplified.

specimen is divided longitudinally into 10 sections, with each section having a different permeability. All research teams results are in good agreement at 1 day and 30 days. The analysis results of the SNL team show inflections that other analysis teams do not have regarding the change in permeability of the specimen, but these inflections are effectively caused by introduced heterogeneity into the modelled samples. However, differences among all research teams are not significant.

As an example of the simulation results, Fig. 21 shows comparisons of teams' modelling results of Step 1–4.

Fig. 21 shows water content distributions. Fig. 21 (a) and (b) show 7 days and 18 days, respectively. The BGR, CAS, JAEA, KAERI, SNL and Taipower teams performed the analysis. All research teams results show good agreement with the laboratory test results. JAEA performed two simulations using different parameters. JAEA-1 uses the parameter set

Table 25
Parameters and boundary conditions for Step 2 (JAEA team).

Team	Parameters and boundary conditions for Step 2
JAEA	[Parameters for Step 2] In Step2 the simulations modeled buffer material, sand layer in the test pit, and backfill material. The parameters of the thermal vapor flow diffusivity was a calibrated parameter based on the test results of Step 1–4. For all parameters the given values were used in the simulation. [Boundary conditions for Step 2] Temperature boundary conditions were set based on measurements of the surface of the simulated overpack and sand layer. Hydraulic boundary conditions were set based on measurements of water injection pressure. These input data were simplified. Displacement outside the sand layer and the backfill material was fixed.

Table 26
Parameters and boundary conditions for Step 2 (KAERI team).

Team	Parameters and boundary conditions for Step 2
KAERI	[Parameters for Step 2] In Step2 the simulations modeled host rock, buffer material, sand layer in the test pit, backfill block, backfill compacted, concrete, simulated overpack and oil in the simulated overpack. Currently, there are no laboratory data related to the BBM and relative permeability of Kunigel®V1. In the case of the BBM properties, a back analysis method was used for parameter identification. The process of the back analysis method consisted of 1) swelling tests, 2) numerical modeling, 3) data acquisition, 4) an artificial neural network (ANN), and 5) multi-objective optimization. For all other parameters the given values were used in the simulation. [Boundary conditions for Step 2] Assuming saturation of the silica sand with groundwater (attributed to its high permeability), the measured pore pressure data from the sand layer were employed as boundary conditions for the surrounding buffer material. The measured temperature sensor data from the sand layer were employed as thermal boundary conditions. The power inputs for each heater were incorporated into the model using provided data. The input data were not simplified.

Table 27
Parameters and boundary conditions for Step 2 (SNL team).

Team	Parameters and boundary conditions for Step 2
SNL	[Parameters for Step 2] In Step2 the simulations represented the host rock, the EDZ, buffer material, sand layer in the test pit, backfill block, compacted backfill, and concrete (plug, roadbed and shotcrete). The buffer material was divided into 3 zones. Full saturation of the buffer was assumed. A thermal conductivity gradient was imposed across the buffer region to fit experimental temperature data. For all other parameters, the values given in the task were used in the simulation. [Boundary conditions for Step 2] Scaling of the provided values and timings of the fluid injection and heating histories was done to account for simplification of the 2-D domain to obtain predictions consistent with temperature and pressure measurements. The scaling mainly applied heating power inputs, fluid injection rates, and thermal conductivities of host-rock and backfilling buffer materials. The water inflow rates used in the model are much lower than those provided by the experimental data. The provided injection flow rates resulted in code run stability issues and unrealistically high pressures. Heating rates as a function of time were also adjusted to match thermocouple temperature measurements.

based on another predictive analysis using TOUGH2, and JAEA-2 uses the calibrated parameter set based on the calibration analysis to these (Step 1–4) laboratory test results. The analytical results of JAEA-2 are in good agreement with the laboratory tests. On the other hand, the analytical results of JAEA-1 show the same trend as the experimental

Table 28
Parameters and boundary conditions for Step 2 (Taipower team).

Team	Parameters and boundary conditions for Step 2
Taipower	[Parameters for Step 2] In Step2 the simulations modeled host rock, buffer material, sand layer in the test pit, backfill block, backfill compacted and concrete (plug, roadbed and shotcrete), simulated overpack and oil in the simulated overpack. For all other parameters the given values were used in the simulation. [Boundary conditions for Step 2] Regarding hydraulic boundary, the original data flow interval was one hour, but an average of one day was used as input data. Assuming that the silica sand was filled with water, the pressure boundary around the buffer material is established. Regarding thermal boundary conditions, the Heat Transfer Module model was used. The full-scale experiment involves two heating devices, referred to as Heater 1 and Heater 2. Heater 2 only operated for five days before stopping, while Heater 1 continued to operate for 2000 days before entering the cooling phase. The source term uses the heater wattage provided by JAEA for the calculation of the thermal model.

results, but overall the simulation results are higher and the difference is greater at the top and bottom ends of the specimen.

This laboratory tests were performed under condition that test cell is nonpermeable. Therefore, simulations were performed considering this condition. However, water content after laboratory tests showed that the saturation of specimen decreased. It is considered that this different of total water content of the specimen between start and end of the laboratory tests is also errors in laboratory tests.

7. Results of step 2

In Step 2, heater system installed in the simulated overpack defines the temperature conditions. The test water injection systems installed in the sand layer around the EBS and in the gallery between the backfill material and concrete support define the hydraulic condition. The research teams set the thermal and hydraulic boundary conditions for simulation of Step 2.

Regarding thermal conditions, some research teams selected temperature and others selected the heater power. When the temperature conditions were selected, each research team developed original conditions because measured data has substantial noise that can cause problems for numerical solvers without improving the representations of the system. Research teams simplified the measured temperature. When the heater power conditions were selected, research teams similarly simplified the measured data.

Fig. 22 shows the thermal (temperature) boundary conditions developed by the research teams. The BGR and CAS team set the temperature on the surface of the simulated overpack. The BGR team set a representative temperature as boundary condition. The CAS team set 10 points as a temperature boundary condition. The JAEA team set 3 points as a prescribed temperature on the surface of the simulated overpack and 2 points in the sand layer.

Fig. 23 shows the thermal (heater power) boundary conditions developed by the research teams. The SNL team set the heater power of both heater 1 and heater 2 as boundary conditions. The Taipower team set a representative heater power as the boundary condition. The KAERI

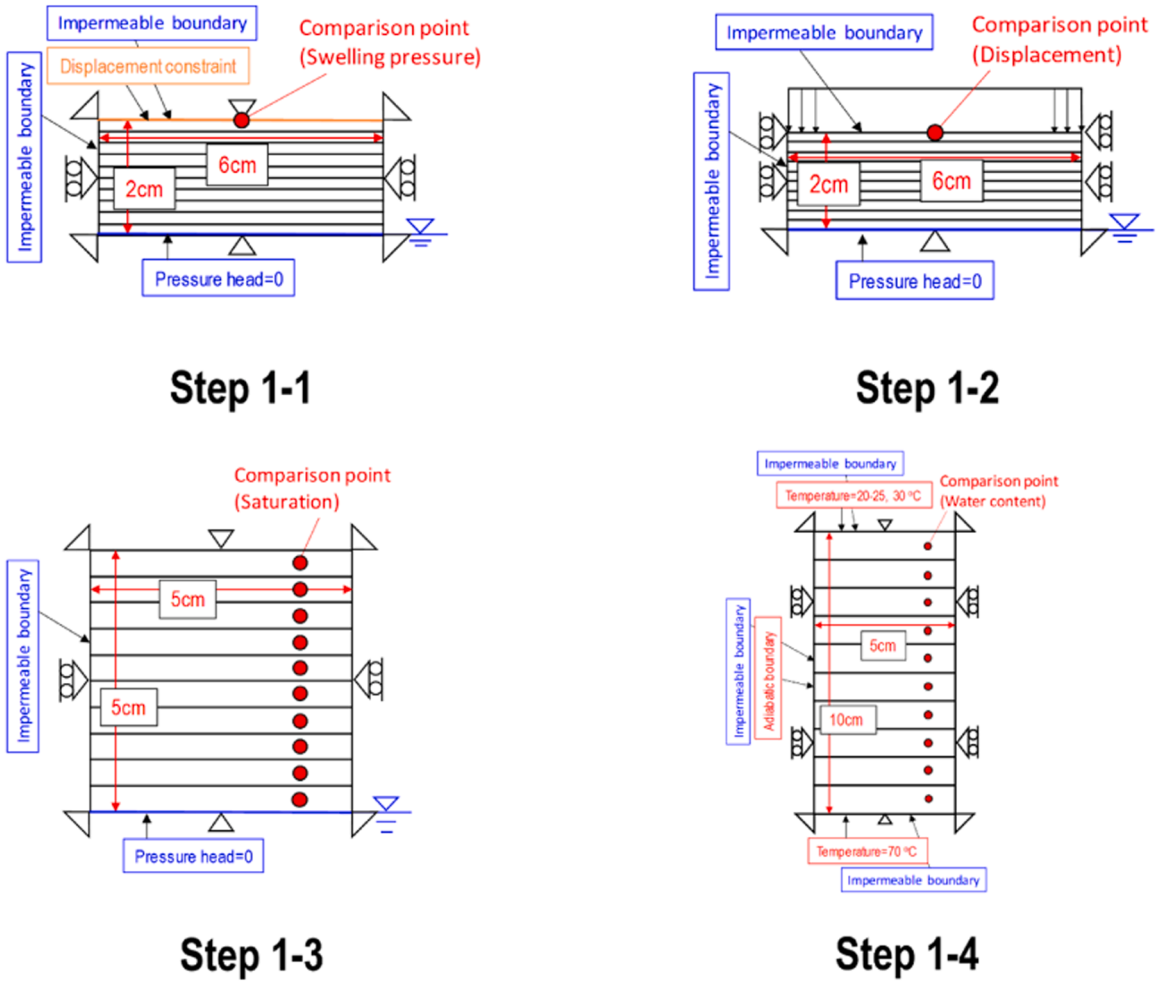

Fig. 17. Images of the benchmark from Step 1–1 to Step 1–4.

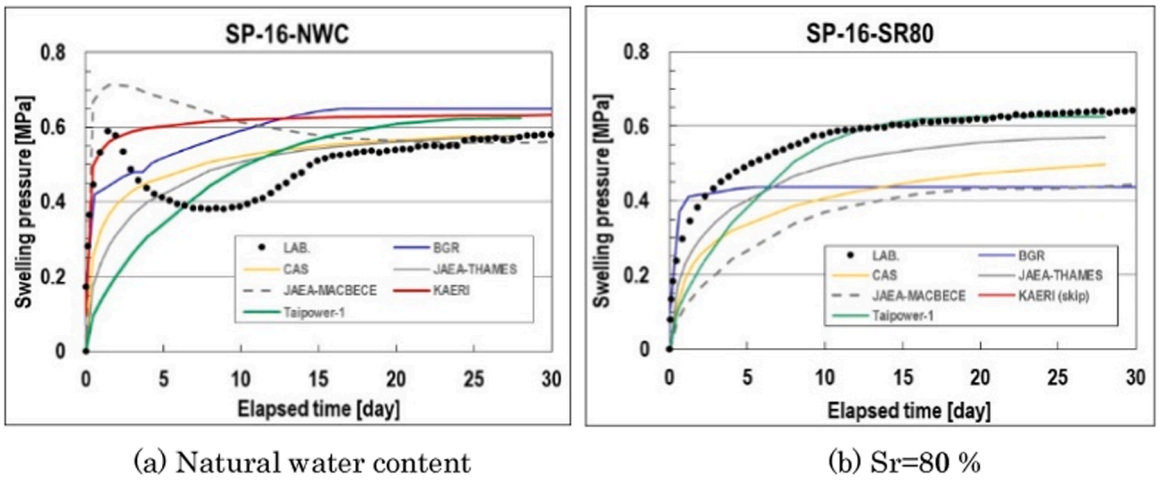

Fig. 18. Comparison of the numerical modelling results on swelling pressure (1.6 Mg/m^3).

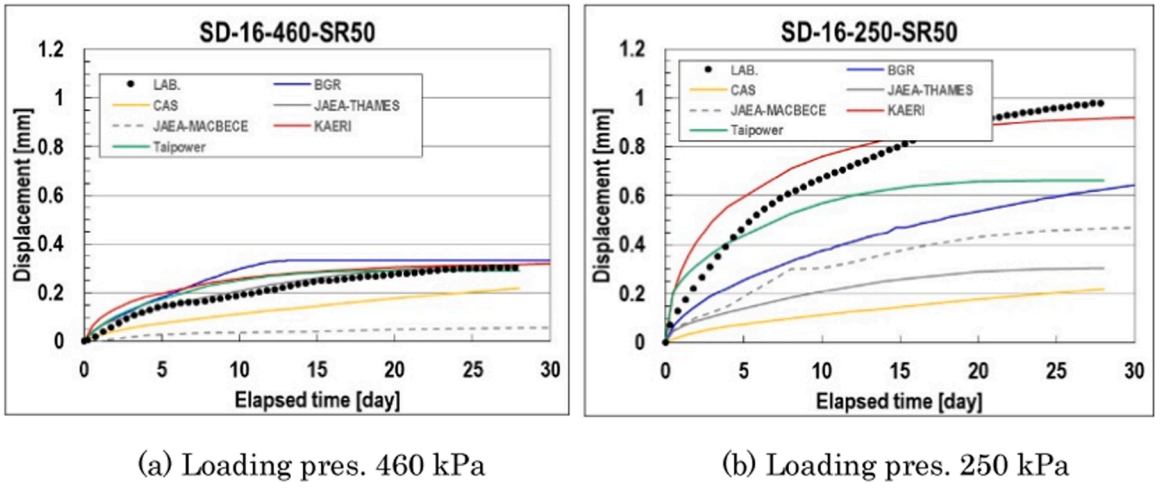

Fig. 19. Comparison of the numerical modelling results on displacement (1.6 Mg/m^3).

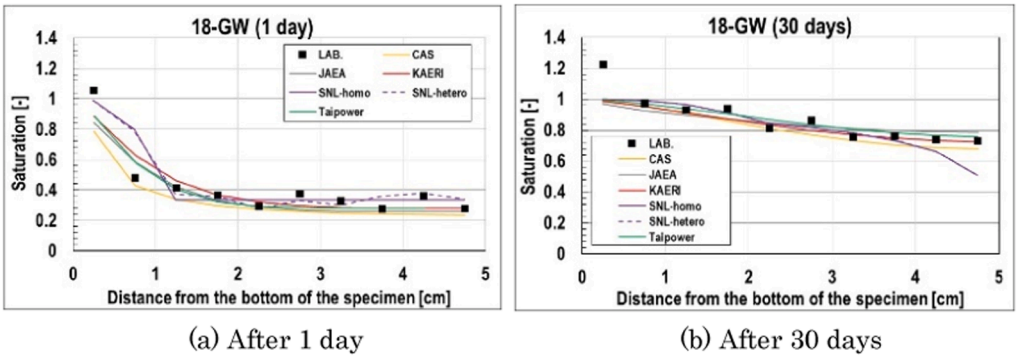

Fig. 20. Comparison of the numerical modelling results on saturation in the specimen (GW).

team set heater power provided by JAEA as the boundary condition. They did not simplify data. Since the heater power data provided by JAEA was very complex, the simulation required a significant amount of calculation time. This is one of the factors why the KAERI team did not perform THM coupling but only TH coupling.

Regarding hydraulic conditions, some research teams selected the injection pressure and others selected the inflow rate. When the injection pressure conditions were selected, each research team developed their own conditions because measured data has considerable noise. Research teams simplified the measured injection pressure. When the inflow rate conditions were selected, research teams similarly simplified the measured data.

Fig. 24 shows the hydraulic (injection pressure) boundary conditions developed by the research teams. The BGR, CAS and JAEA team set both injection pressures of the pit injection system and the gallery injection system as boundary conditions. The Taipower team set the injection

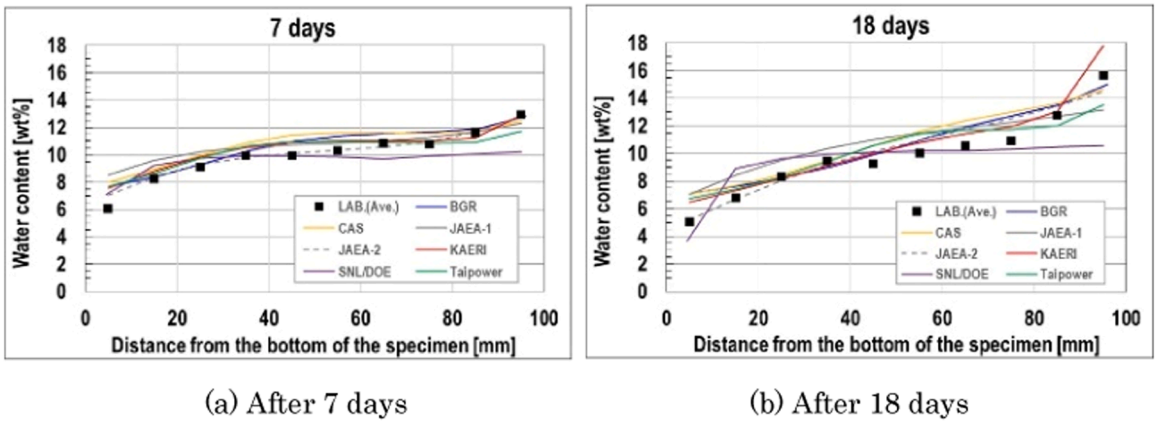

Fig. 21. Comparison of the numerical modelling results on water content in the specimen.

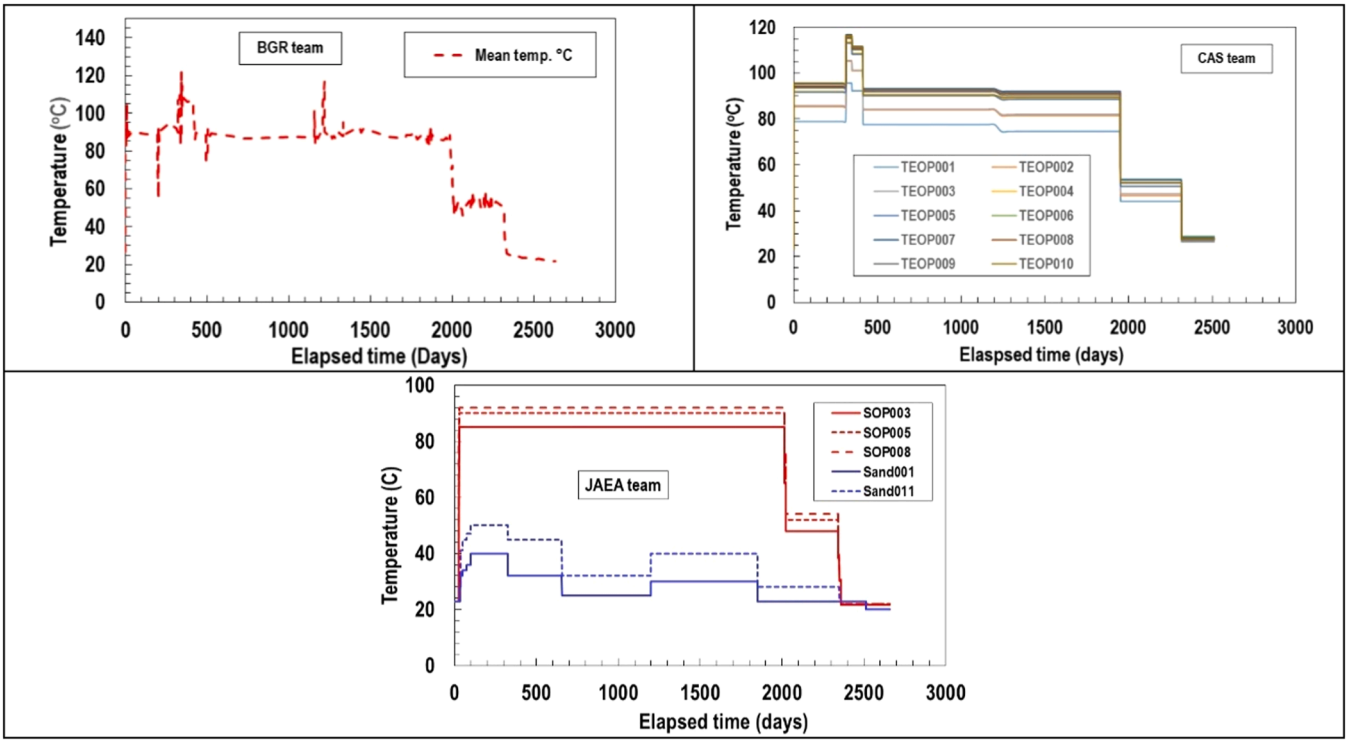

Fig. 22. Thermal boundary conditions developed by the research teams (Temperature).

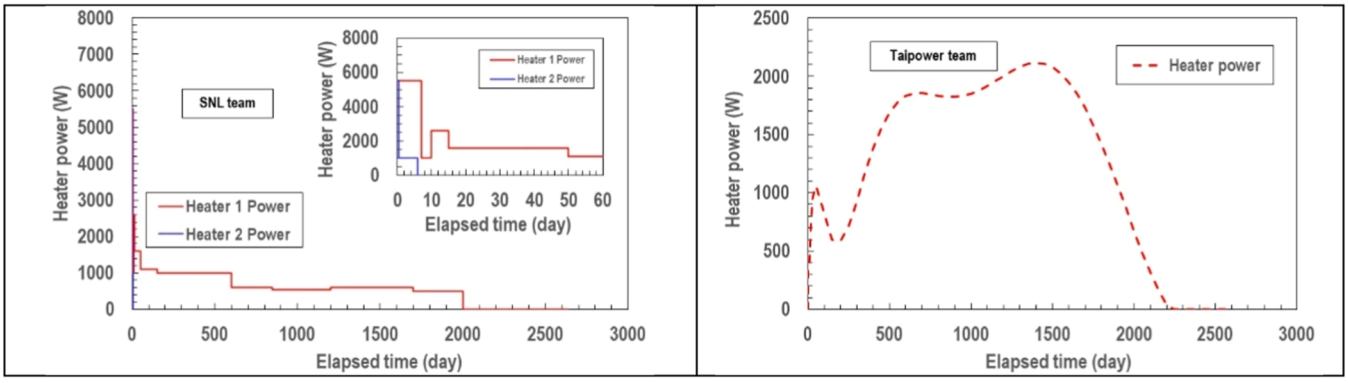

Fig. 23. Thermal boundary conditions developed by the research teams (Heater power).

pressure of the pit injection system and also set an inflow rate, too (see Fig. 25). The KAERI team set the injection pressure in the gallery injection system provided by JAEA as boundary condition. They did not simplify the data. Since the injection pressure data provided by JAEA was very complex, the simulation required a significant amount of calculation time. This is one of the factors why the KAERI team did not perform THM coupling but only TH coupling.

Fig. 25 shows the hydraulic (inflow rate) boundary conditions developed by the research teams. The SNL team set the inflow rate of both the pit and the gallery as a boundary condition.

Fig. 26 shows the analytical meshes for the Step 2 developed by all research teams. The obvious differences are 2D / 3D, EBS with the gallery / EBS with the gallery and rock mass.

Figure 27 shows comparison points between simulation results and measured data in Step 2. This is the cross section of the centre of the EBS (on the longitudinal centre of the simulated overpack). These comparison points compare temperature, saturation (water content) and total pressure. The displacement comparison point is located under the simulated overpack.

In the Horonobe EBS experiment, the hydraulic behaviour of the buffer material was measured using a psychrometer and a hygrometer. A psychrometer is suitable for measuring humid conditions, where water content is high, and a hygrometer is suitable for measuring dry conditions, where water content is low. Unfortunately, the hygrometer did not work properly. For this reason, it was almost impossible to measure the water content in the dryer state.

Therefore, comparisons of the numerical modelling results on temperature, saturation, total pressure in the outer part of the buffer material are discussed.

Comparisons of teams' modelling results of Step 2 (temperature) are shown in Fig. 28 (temperature evolution with the elapsed time). All research teams performed the analysis, especially tendency of evolutions. There are some variations among research teams. It is considered that boundary conditions research teams developed/simplified caused such variation of the temperature distributions in the buffer material.

Fig. 29 shows suction evolution with the elapsed time. Outside of the buffer material, all research teams performed the analysis. Although the analysis results showed different paths of increase of the suction from the start of the heating phase, the increasing trend of all research teams was broadly consistent with the measurement data.

Comparisons of teams' modelling results of Step 2 (total pressure) are shown in Fig. 30.

Fig. 30 shows total pressure evolution with the elapsed time. Outside of the buffer material, all research teams that performed coupled THM analysis presented the analysis results. Although the analysis results showed difference paths of increase of the pressure from the start of the heating phase, the value of the total pressure after increasing for all research teams were consistent with the measurement data.

8. Conclusion

In this contribution we will show a synthesis of the team results for the laboratory test as well as for the Horonobe EBS experiment. In Step 1, the approach was slightly different for each research team, the major difference was whether to apply the elastic model or the elasto-plastic model to the mechanical model. In Step 2, there were differences in the coupled THM model, and there were also differences in how to consider the boundary conditions.

Task D validated various approaches thorough the simulation of the in-situ full scale EBS system including backfill of the gallery: variations in the coupling processes (THM or THC), analysis codes, and boundary conditions.

Six research teams (BGR, CAS, JAEA, KAERI, SNL and Taipower) participated the Task D. BGR, CAS, JAEA, KAERI and Taipower research teams selected a THM approach, while the SNL research team selected a TH approach.

8.1. Parameter identification

The stepwise approach of Step 1 (laboratory tests) preceding Step 2 (In-situ test) was an ideal structure for Task D.

The simulation of the coupled THM behaviour analysis requires

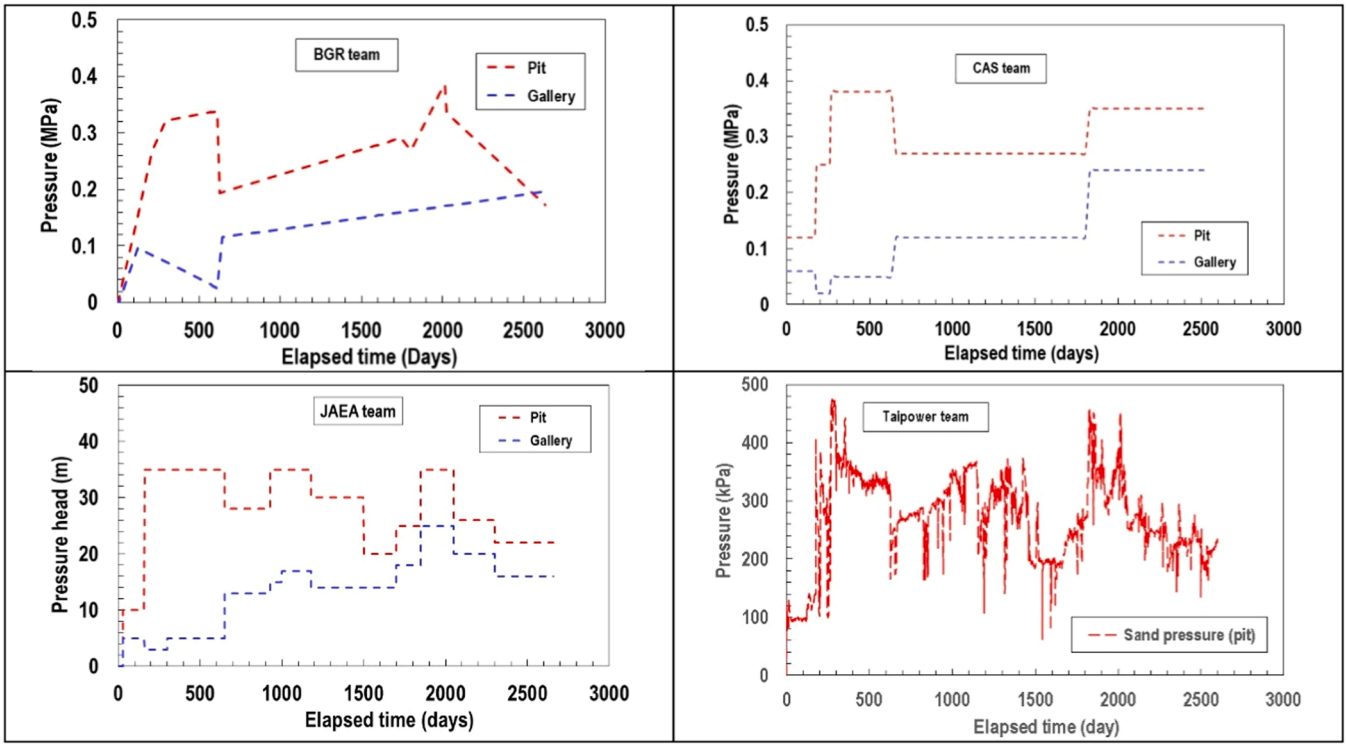

Fig. 24. Hydraulic boundary conditions developed by the research teams (Injection pressure).

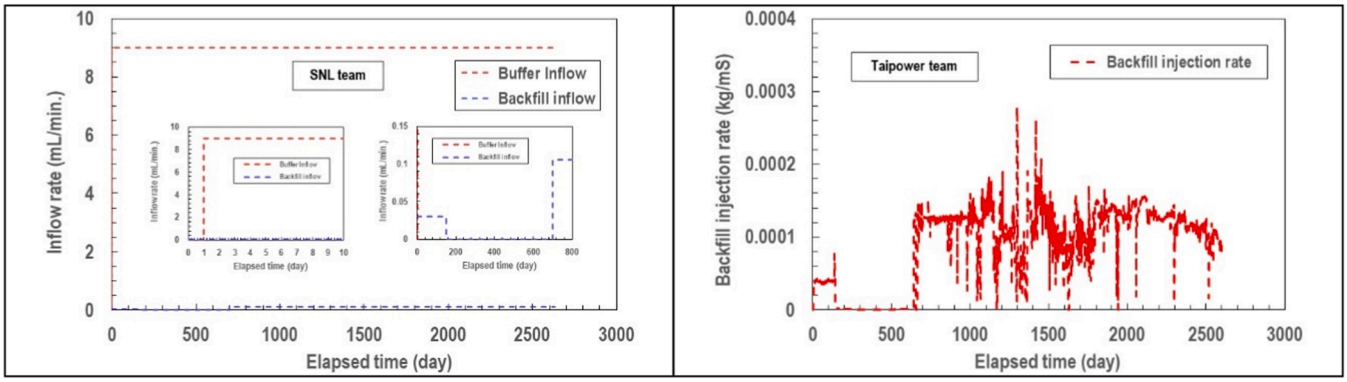

Fig. 25. Hydraulic boundary conditions developed by the research teams (Inflow rate).

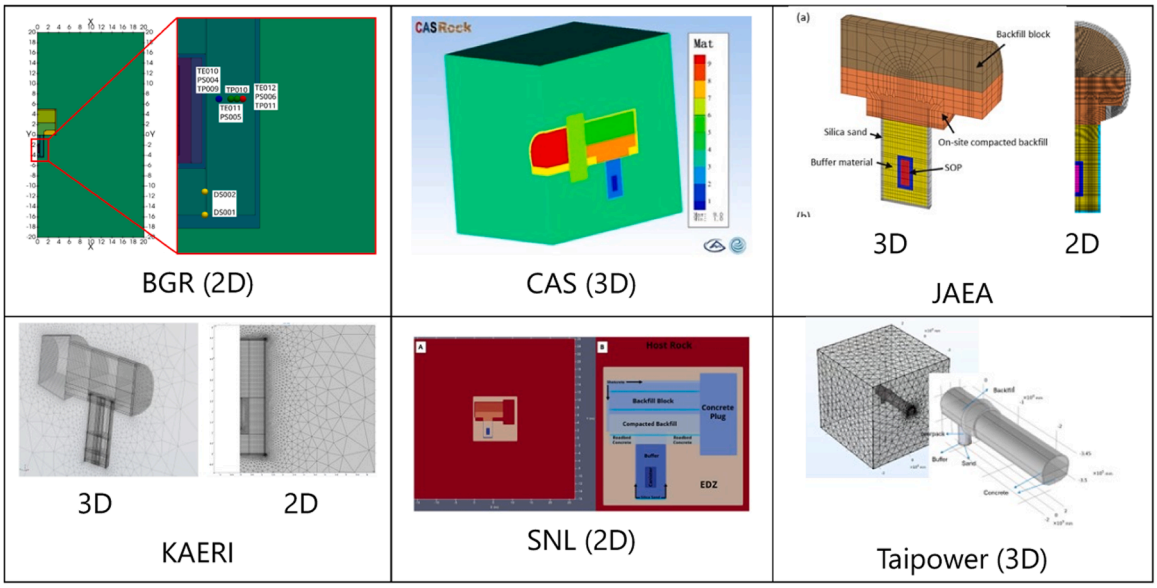

Fig. 26. Analytical mesh for the Step 2.

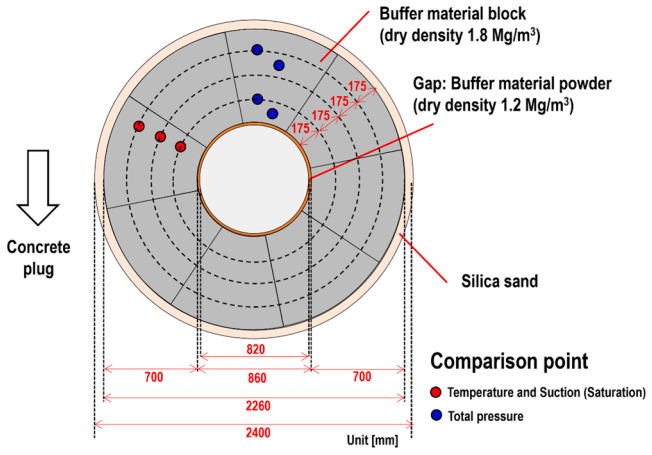

Fig. 27. Comparison points in Step 2.

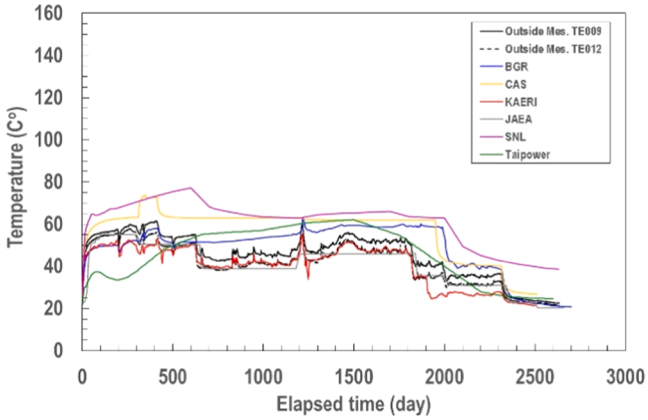

Fig. 28. Comparison of the numerical modelling results on temperature in Step 2.

various parameters. Some preliminary simulations using results from simple coupled laboratory tests are useful to check and validate candidate parameters.

Special parameters required by a particular analysis numerical code can usually be identified by back analysis of the laboratory tests results. For example, unknown properties (BBM parameters and relative permeability of liquid and gas) were characterized using the back analysis method and parametric studies.

In the case of parameters which are difficult to derive through direct experiments, the choice of these parameters can significantly impact the

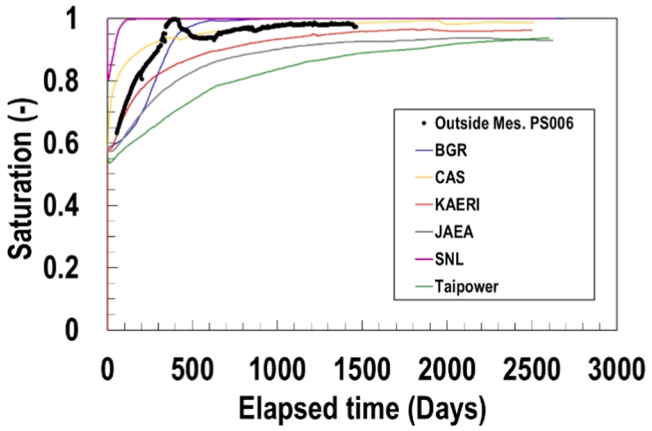

Fig. 29. Comparison of the numerical modelling results on saturation in Step 2.

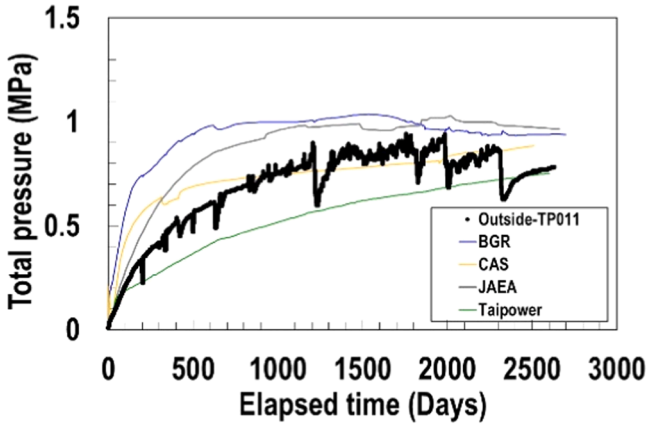

Fig. 30. Comparison of the numerical modelling results on total pressure in Step 2.

results. (e.g. relative gas permeability). Therefore, it is necessary to obtain all parameters through indirect methods, (i.e. experiments + parameter identification techniques), before the simulation work of the in-situ experiments.

8.2. Boundary conditions

In simulation of the EBS system, boundary conditions for the heating element and water injection were defined using measured data as Dirichlet boundaries using temperature and water pressure. Ideally, power or flow rate data would align simulations more closely with more realistic conditions in future studies as these are the true boundary conditions for the system. The waste package is a heating element that generates heat from decay heat during radioactive decay, hence the true boundary is a heat flux. On the other hand, there are two possibilities for hydraulic boundary conditions: injection pressure and flow rate. At the repository, it is conceivable to monitor the injection pressure with a pressure gauge installed in the borehole, and measure the flow rate (volume) with a flowmeter set in the gallery. While it is possible to construct a boundary that reflects the complexity of the hydraulic boundary condition for the in-situ test, not all codes have the capability to represent such boundaries.

In all cases where the boundaries applied are somewhat artificial or prescribed, it is important that a wider search of the model behaviour is conducted to check whether the global model behaviour is plausible. For example, when specifying temperature on the heater surface it is important to compare the calculated heat flux with the known heat input to the system. If the fluxes diverge while the temperatures are consistent it reveals a more general issue with the model.

8.3. Swelling of the material (buffer material and backfill material)

The application of an elasto-plastic constitutive model to the mechanical model of the buffer material has improved the reproducibility of the swelling behaviour of the buffer material. When an elastic constitutive model is applied, adding an equation for considering swelling displacement can also simulate deformation well, for example JAEA team applied.

8.4. 2D and 3D

Realization of the 3D simulation for the EBS experiment was impeded due to the computational demand imposed by the constitutive equations, which increases simulation times drastically. As a result, the simulation of the EBS experiment of some research teams was instead performed using a 2D axisymmetric model or a 2D plane strain model.

Experience from this task and other tasks shows that even a minor difference in input data can lead to very different results for these complex coupled problems. Therefore, when performing interpolation or making assumptions, it is important to check whether such simplifications have an impact or not. Simplified 2D representations of the system can be adequate but requires careful assumptions to produce output that is directly comparable to the data.

8.5. Other points

Temperature distribution in the buffer material was simulated well by all research teams. In this task (both Step 1 n and Step 2) all materials considered are in contact with each other. There is no need to model gaps in the model. In such a case, the thermal behaviour is considered to be insensitive to the simulation approaches.

The water content distribution on the outside of the buffer material was well simulated by all research teams. In the Horonobe EBS experiment, measured values suitable for validating the simulation results were not obtained near the simulated overpack.

When simulating the pressure of the buffer material, the measurement data is easily affected by the installation conditions of the measurement sensors, so verifying the measurement data itself remains an issue. Mechanical simulation results differ depending on whether they are considered as elastic or elastoplastic phenomena.

The accuracy of measured in-situ data can be assessed by detailed analysis comparing sampling specimen analysis and measured data. The Horonobe EBS experiment is scheduled to be dismantled in the future (FY2026 and 2027). This detailed dismantling investigation will finally confirm the measured data.

CRediT authorship contribution statement

Lopez Carlos M: Writing – original draft. **Jove-Colon Carlos:** Writing – original draft. **Liang Suu-yan:** Writing – original draft. **Pan Pengzhi:** Writing – original draft. **Beese Steffen:** Writing – original draft. **Lee Changsoo:** Writing – original draft. **Kim Minseop:** Writing – original draft. **Ohno Hirokazu:** Writing – original draft. **Sugita Yutaka:** Writing – review & editing, Writing – original draft, Conceptualization.

Declaration of Competing Interest

The authors declare that they have no known competing financial interests or personal relationships that could have appeared to influence the work reported in this paper.

Acknowledgement

DECOVALEX is an international research project comprising

participants from industry, government and academia, focusing on development of understanding, models and codes in complex coupled problems in sub-surface geological and engineering applications; DECOVALEX-2023 is the current phase of the project. The authors appreciate and thank the DECOVALEX-2023 Funding Organisations Andra, BASE, BGE, BGR, CAS, CNSC, COVRA, US DOE, ENRESA, ENSI, JAEA, KAERI, NWMO, NWS, SÚRAO, SSM and Taipower for their financial and technical support of the work described in this paper. The statements made in the paper are, however, solely those of the authors and do not necessarily reflect those of the Funding Organisations.

CAS team's work was financially supported by National Natural Science Foundation of China (Grant No. 52339001)

KAERI team's work was also supported by the Institute for Korea Spent Nuclear Fuel (iKSNF) and National Research Foundation of Korea (NRF) grant (2021M2E1A1085193), and the Nuclear Research and Development Program of the National Research Foundation of Korea (NRF) (2021M2E3A2041351) funded by the Korean government (Ministry of Science and ICT, MSIT).

Sandia National Laboratories is a multi-mission laboratory managed and operated by National Technology and Engineering Solutions of Sandia LLC, a wholly owned subsidiary of Honeywell International Inc. for the U.S. Department of Energy's National Nuclear Security Administration under contract DE-NA0003525. The views expressed in the article do not necessarily represent the views of the U.S. DOE or the United States Government. No inferences should be drawn from this document regarding future actions by DOE, which are limited both by the terms of the Standard Contract and Congressional appropriations for the Department to fulfill its obligations under the Nuclear Waste Policy Act including licensing and construction of a spent nuclear fuel repository. This work was supported by the DOE-NE SFWST program.

Data Availability

The data that has been used is confidential.

References

1. NUMO. 2021. The NUMO Pre-siting SDM-based Safety Case, NUMO-TR-21-01.
2. JNC. 2000. Second progress report on research and development for the geological disposal of HLW in Japan, H12: Project to establish the scientific and technical basis for HLW disposal in Japan, Supporting report 2 Repository design and engineering technology, JNC TN1400 2000-003.
3. Bundesministerium für Umwelt, Naturschutz, Bau und Reaktorsicherheit (BMUB). 2017. Standortauswahlgesetz vom 5. Mai 2017 (BGBl. I S. 1074), which was last amended by Article 8 of the Act of March 22, 2023 (BGBl. 2023 I Nr. 88).
4. Jobmann M, Bebiolka A, Burlaka V, et al. Safety assessment methodology for a German high-level waste repository in clay formations. *J Rock Mech Geotech Eng.* 2017;9(5):856–876. DOI:10.1016/j.jrmge.2017.05.007.
5. Jobmann, M. and Burlaka, V. 2021. Verfüll- und Verschlusskonzepte für Endlager im Kristallingestein in Deutschland. BGE TECHNOLOGY GmbH, Technischer Bericht, BGE TEC 2021-15. Forschungsprojekt CHRISTA II; Peine.
6. Wang J, Chen L, Su R, Zhao X. "The Beishan underground research laboratory for geological disposal of high-level radioactive waste in China: Planning, site selection, site characterization and in situ tests. *J Rock Mech Geotech Eng.* 2018;10(3):411–435.
7. Chen L, Zhao X, Liu J, et al. "Progress on rock mechanics research of Beishan granite for geological disposal of high-level radioactive waste in China. *Rock Mech Bull.* 2023;2(3), 100046.
8. Lee, J.Y., Kim, I.Y., Ju, H.J. and Cho, D.K. 2020. Proposal of an Improved Concept Design for the Deep Geological Disposal System of Spent Nuclear Fuel in Korea, JNFCWT V.18 No. S.
9. Lee J, Kim K, Kim I, et al. High-efficiency deep geological repository system for spent nuclear fuel in Korea with optimized decay heat in a disposal canister and increased thermal limit of bentonite. *Nucl Eng Technol.* 2023;55(4):1540–1554.
10. Swift PN, Bonano EJ. Geological disposal of nuclear waste in tuff: Yucca Mountain (USA). *Elements.* 2016;12:263–268.
11. Stein E, Bryan CR, Dobson DC, et al. Disposal Concepts for a High-Temperature Repository in Shale (SAND2020-12471R). *Sandia Natl Lab, Albuq, NM (U S), Albuq, NM USA.* 2020:160.
12. Taipower. *The Spent Nuclear Fuel Final Disposal Program—Preliminary Development of Pre-Siting Safety Case.* Taiwan Power Company; 2023 (Taipower).
13. Nakayama, M., Matsuzaki, T. and Niunoya, S. 2016. The in-situ experiment for performance confirmation of engineered barrier system at Horonobe underground research laboratory - production of casting drilling machine for large diameter pit, simulated overpack, buffer material blocks and backfilling materials -, JAEA-Research 2016-010. DOI: 10,11484/jaea-research-2016-010 (in Japanese).
14. Nakayama, M. and Ohno, H. 2019. The in-situ experiment for performance confirmation of engineered barrier system at Horonobe underground research laboratory - installation of engineered barrier system and backfilling the test niche at the 350m gallery -, JAEA-Research 2019-007. DOI: 10,11484/jaea-research-2019-007 (in Japanese).
15. Sugita, Y., Beese, S., Maßmann, J., Pan, P., Kim, M., Lee, C., Ohno, H., Ozaki, Y., Jové Colón, C.F., Lopez, C.M. and Liang, S. 2024. DECOVALEX-2023 Task D Final Report.
16. Suzuki, H. and Takayama, Y. 2020. Impact Assessment of Density Change on the Buffer Material on the Coupled Thermal-Hydraulic and Mechanical (THM) Behavior in the Near-field, JAEA Research 2020-015. DOI: 10.11484/jaea-research-2020-015 (in Japanese).
17. Japan Atomic Energy Agency and Radioactive Waste Management Funding and Research Center. 2019. The project for validating near-field system assessment methodology in geological disposal Annual report for JFY2019 (in Japanese).
18. Nakayama M. (Ed.) 2024. Horonobe Underground Research Laboratory Project Investigation Report for the 2022 Fiscal Year, JAEA-Review 2023-032. DOI: 10.11484/jaea-review-2023-032 (in Japanese).
19. Matsumoto, K., Kanno, T., Fujita, T. and Suzuki, H. 1997. Saturation hydraulic properties of the buffer material, PNCTN8410 97-296 (in Japanese).
20. Kikuchi, H., Tani, K., Matsumoto, K., Sato H., Ueno, K., and Tetsu, T. 2003. Hydraulic characteristics of buffer material-II; The influence which saline water exert on hydraulic properties of bentonite buffer material, JNC TN8430 2003-002 (in Japanese).
21. Kikuchi, H. and Tanai, K. 2004. Basic Characteristic Test of Buffer / Backfill Material under Horonobe Groundwater Condition, JNC TN8430 2004-005 (in Japanese).
22. van Genuchten MT. A Closed-form Equation for Predicting the Hydraulic Conductivity of Unsaturated Soils. *Soil Sci Soc Am J.* 1980;44:892–898.
23. Bilke L, Flemisch B, Kalbacher T, Kolditz O, Helmig R, Nagel T. Development of open-source porous media simulators: Principles and experiences. *Transp Porous Media.* 2019;130:337–361.
24. Feng XT, Pan PZ, Zhou H. Simulation of the rock microfracturing process under uniaxial compression using an elasto-plastic cellular automaton. *Int J Rock Mech Min Sci.* 2006;43-7:1091–1108.
25. Pan PZ, Feng XT, Hudson J. A. Study of failure and scale effects in rocks under uniaxial compression using 3D cellular automata. *Int J Rock Mech Min Sci.* 2009;46-4:674–685.
26. Ohnishi Y, Shibata H, Kobayashi A. Development of finite element code for the analysis of coupled thermo-hydro-mechanical behaviours of a saturated-unsaturated medium. *Proc Int Symp Couple Process Affect Perform a Nucl Waste Repos, Berkeley.* 1985:263–268.
27. Mihara M, Hirano F, Takayama Y, Kyokawa H, Ohno S. Long-term mechanical analysis code considering chemical alteration for a TRU waste geological repositor. *J Nucl Fuel Cycle Environ.* 2017;24(1):15–26.
28. COMSOL Inc, 2020. COMSOL Multiphysics LiveLink For MATLAB Users Guide (version 5.6). In Comsol.
29. Lichtner, P.C., Hammond, G.E., Lu, C., Karra, S., Bisht, G., Andre, B., Mills, R.T., Kumar, J., and Frederick, J.M. 2020. PFLOTRAN User Manual, Technical Report (⟨https://www.pflotran.org/⟩).
30. COMSOL Multiphysics® v. 5.6. www.comsol.com. COMSOL AB, Stockholm, Sweden.
31. Richards LA. Capillary conduction of liquids through porous mediums. *Physics.* 1931;1(5):318–333.
32. Callari C, Auricchio F, Sacco E. A finite-strain cam-clay model in the framework of multiplicative elasto-plasticity. *Int J Plast.* 1998;14(12):1155–1187.
33. Chijimatsu M, Fujita T, Kobayashi A, Nakano M. Experiment and validation of numerical simulation of coupled thermal, hydraulic and mechanical behaviour in the engineered buffer materials. *Int J Numer Anal Meth Geomech.* 2000;24:403–424.
34. Chijimatsu, M. Fujita, T. Sugita, Y. Amemiya, K. and Kobayashi, A. 2000b. In-Situ Coupled Thermo-Hydro-Mechanical Experiment at Kamaishi Mine, Int. Conf. on Geotechnical & Geological Engineering (GeoEng2000), Int. Soc. for Rock Mechanics, etc.
35. Börgesson, L. and Hernelind, J., 1999. Coupled thermo-hydro-mechanical calculations of the water saturation phase of a KBS-3 deposition hole. TR-99-41.
36. Japan Atomic Energy Agency and Radioactive Waste Management Funding and Research Center. 2021. The project for validating near-field system assessment methodology in geological disposal Annual report for JFY2020, 533 (in Japanese).
37. Ohno S, Kawai K, Tachibana S. Elasto-plastic constitutive model for unsaturated soil applied effective degree of saturation as a parameter expressing stiffness. *J JSCE.* 2007;63(4):1132–1141.
38. Takayama Y, Tachibana S, Iizuka A, Kawai K, Kobayashi I. Constitutive modeling for compacted bentonite buffer materials as unsaturated and saturated porous media. *Soils Found.* 2017;57(1):80–91.
39. Kim MS, Jeon JS, Kim MJ, Lee J, Lee SR. A multi-objective optimization of initial conditions in a radioactive waste repository by numerical thermo-hydro-mechanical modeling. *Comput Geotech.* 2019;114, 103106.
40. Alonso EE, Gens A, Josa A. A constitutive model for partially saturated soils. *Géotechnique.* 1990;40(3):405–430.
41. Wang Q, Tang AM, Cui YJ, Barnichon JD, Ye WM. Investigation of the hydro-mechanical behaviour of compacted bentonite/sand mixture based on the BExM model. *Comput Geotech.* 2013;54:46–52.
42. Roscoe, K., Burland, J.B., 1968. On the generalized stress-strain behaviour of wet clay. The National Academies of Sciences, Engineering, and Medicine.
43. Villar, M., Sánchez, M. and Gens, A. 2008. Behaviour of a bentonite barrier in the laboratory: experimental results up to 8 years and numerical simulation. Physics and Chemistry of the Earth, Parts A/B/C 33, S476-S485.

44. Meleshyn AY, Zakusin SV, Krupskaya VV. Swelling pressure and permeability of compacted bentonite from 10th khutor deposit (Russia). *Minerals*. 2021;11:742.
45. Adams, B.M., Bohnhoff, W.J., Dalbey, K.R., Ebeida, M.S., Eddy, J.P., Eldred, M.S., Hooper, R.W., Hough, P.D., Hu, K.T., Jakeman, J.D., Khalil, M., Maupin, K.A., Monschke, J.A., Ridgway, E.M., Rushdi, Ahmad A., Seidl, D.T., Stephens, J.A., and Winokur, J.G. 2021. "Dakota, A Multilevel Parallel Object-Oriented Framework for Design Optimization, Parameter Estimation, Uncertainty Quantification, and Sensitivity Analysis: Version 6.15 User's Manual". Sandia National Laboratories, United States. https://doi.org/10.2172/1829573. ⟨https://www.osti.gov/servlets/purl/1829573⟩.
46. Bear J. *Dynamics of Fluids in Porous Media*. Elsevier Scientific Publishing; 1972.
47. He Y. Moisture absorption and hygroscopic swelling behavior of an underfill material. *Thermochim Acta*. 2012;546:143–152.
48. Nield DA, Bejan A. *Convection in porous media*. 3. New York: springer; 2006:629–982.
49. Antoine C. Tensions des vapeurs; nouvelle relation entre les tensions et les températures. *Comptes Rendus Des Séances De l'Académie Des Sci*. 1888;107:681–684.
50. He Y. Moisture absorption and hygroscopic swelling behavior of an underfill material. *Thermochim Acta*. 2012;546:143–152.
51. Bear J. *Dynamics of Fluids in Porous Media*. Amsterdam: Elsevier; 1988.
52. Pan P-Z, Yan F, Feng X-T, Wu Z-H. Study on coupled thermo-hydro-mechanical processes in column bentonite test. *Environmental Earth Sciences*. 2017;76(17):618.